

A FULL SCALE ROOM FOR THE EXPERIMENTAL STUDY
OF INTERIOR BUILDING CONVECTIVE HEAT
TRANSFER: DESIGN AND VALIDATION

By
JEFFERY DON FERGUSON
Bachelor of Science
Oklahoma State University
Stillwater, Oklahoma
1991

Submitted to the Faculty of the
Graduate College of the
Oklahoma State University
in partial fulfillment of
the requirements for
the Degree of
MASTER OF SCIENCE
May 1997

Name: Jeffery D. Ferguson

Date of Degree: May, 1997

Institution: Oklahoma State University

Location: Stillwater, Oklahoma

Title of Study: A FULL SCALE ROOM FOR THE EXPERIMENTAL STUDY OF
INTERIOR BUILDING CONVECTIVE HEAT TRANSFER: DESIGN
AND VALIDATION

Pages in Study: 109

Candidate for the Degree of Master of Science

Major Field: Mechanical Engineering


Scope and Method of Study: The purpose of this work was to design, build, and validate an experimental room for the study of building interior convective heat transfer. The full-scale room with interior dimensions 16'x12'x10', was constructed with 18" walls and 15" floor and ceiling. The facility was elevated 5' above the lab floor and the walls were heavily insulated. All six surfaces were divided into 2'x4' cells with a unique modular heated panel system mounted on the inside of the cells. ASHRAE Standard 51 was employed for volumetric air flow measurement. A water source heat pump provided chilled water to a fan-coil unit which in turn provided conditioned air to the room. A total of seventeen validation tests were performed focusing on volumetric air flow measurement and an overall room heat balance. Analysis was directed at results from a subset of seven experiments ranging from 5-25 ach. Additionally, an uncertainty analysis was performed for all experiments.

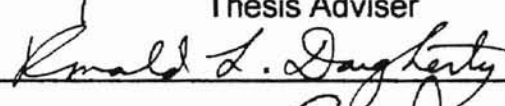
Findings and Conclusions: For the lower volumetric experiments (<10 ach), initial room heat balance results, coupled with the uncertainty results, fell short of good agreement. Further analysis isolated uncertainty sources at the room inlet temperature measurement, radiative communication with room inlet temperature measurement, room conduction backlosses and room transient effects. Recommendations are given to alleviate these uncertainties. Suggestions for future work and research, that the experimental facility could support, are given. The room, while operational, will require further testing, modification and evaluation to be considered a viable building interior convective heat transfer investigative facility.

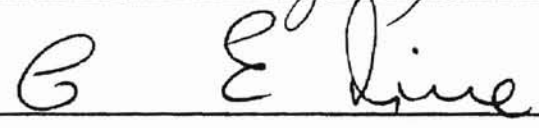
ADVISER'S APPROVAL: _____


A FULL SCALE ROOM FOR THE EXPERIMENTAL STUDY
OF INTERIOR BUILDING CONVECTIVE HEAT
TRANSFER: DESIGN AND VALIDATION

Thesis Approved:



Thesis Adviser






Dean of the Graduate College

ACKNOWLEDGMENTS

I would first of all like to thank my advisor, Dr. Jeffrey Spitler. As a professor and mentor his guidance, support and understanding over the last four years have been invaluable and crucial in the completion of this work.

I would also like to thank the following graduate and undergraduate students: Scott Sanders, fellow office mate and graduate student for his assistance, technical and practical, in the construction of this entire facility; Tony Timko, for his thorough research, design, and analysis of the air flow measurement box and chiller control box; Darrell Dougherty, for his construction expertise and dogged determination to build a safe, sound experimental structure, and work study Richard Page for his carpentry know-how and willingness each week to do whatever was needed. The above mentioned students were great to work with and all had a tremendous part in getting this facility constructed. I would also like to thank Tom Crowell for bringing to this project his electrical wiring expertise. Finally, a special thanks is extended to Tony Rice for his computer-aided design expertise in drafting a three-dimensional model of the experimental room.

Financial support for this project was provided by the University Center for Energy Research. Their financial backing was greatly appreciated. Others

supporting this project through equipment donations, administrative assistance, and facility and laboratory use were: Dr. R.L. Lowery, Dr. A.J. Ghajar, Dr. James Bose, and Dr. L.L. Hoberock. Special thanks also goes to members of my review committee, Dr. C.E. Price and Dr. R.L. Dougherty for their insightful critique and comments for implementation into my final draft.

Heartfelt thanks goes to my parents, Donnie and Karen Ferguson, for their patience, loving support, financial and spiritual backing, and their understanding during the course of my undergraduate and graduate education. Finally, I want to thank my wife Amy Ferguson and my two daughters, Torie and Taylor for putting up with many late nights at the lab and home, for their love and support and for encouraging me to press on to bring this project to completion.

TABLE OF CONTENTS

Chapter, Section	Page
1. INTRODUCTION.....	1
1.1 Background.....	1
1.2 Literature Review.....	1
1.2.1 Full Scale Facilities.....	4
1.2.2 Scale Models.....	10
1.3 Objectives.....	16
2. EXPERIMENTAL FACILITY.....	18
2.1 Overview of Experimental Facility.....	18
2.2 Room Description.....	20
2.2.1 Modular Heated Panel System.....	24
2.2.2 Room Instrumentation and Controls.....	25
2.3 Air System Description.....	26

TABLE OF CONTENTS CONTINUED

Chapter,Section	..Page
2.3.1 Fan-Coil Unit.....	26
2.3.2 Air Flow Measurement Box.....	27
2.3.3 Reheat Coil.....	32
2.3.4 Ducting.....	33
2.4 Chilled Water System.....	34
2.4.1 Chiller Controls.....	34
2.5 Air Side Instrumentation.....	36
2.6..Data Acquisition.....	36
2.7..Experimental Procedure.....	37
2.7.1 Experimental Startup and Shutdown.....	41
2.8 Experimental Uncertainties.....	42
2.8.1 Volumetric Flow Rate Uncertainty.....	42

TABLE OF CONTENTS CONTINUED

Chapter,Section	..Page
2.8.2 Temperature Measurement Uncertainty.....	43
2.8.3 Panel Power Uncertainty.....	44
2.8.4 Spatial Average Uncertainty.....	44
3. RESULTS AND ANALYSIS.....	47
3.1 Summary of Experiments.....	47
3.1.1 Data Analysis.....	48
3.1.2 Experimental Averages.....	49
3.2 Transient Versus Steady State.....	51
3.3 Room Heat Balance.....	62
3.3.1 Air Heat Gain Uncertainty.....	62
3.3.2 Preliminary Heat Balance Results.....	64
3.3.3 Room Inlet Factors.....	66

TABLE OF CONTENTS CONTINUED

Chapter, Section	..Page
3.3.3.1 Temperature and Velocity Gradient.....	66
3.3.3.2 Radiation Effects.....	67
3.3.4 Air Heat Gain Modification.....	72
3.3.4.1 Room Transient Effects.....	72
3.3.4.2 Room Conduction Backlosses.....	74
3.3.5 Modified Heat Balance Results.....	75
4. SUMMARY AND RECOMMENDATIONS.....	78
BIBLIOGRAPHY.....	81
APPENDICES.....	83

LIST OF TABLES

Table	Page
1.1 An Overview of Convective Heat Transfer Experiments.....	3
2.1 Fan-Coil Unit Performance.....	27
2.2 Experimental Sequence: Instantaneous Status Log.....	40
3.1 Overview of Experiments.....	48
3.2 Average Temperatures.....	50
3.3 Average Air Properties.....	51
3.4 Heated Panel Power Duty Cycles.....	54
3.5 Air Heat Gain Uncertainty by Experiment.....	64
3.6 Summary of Panel Power and Air Heat Gain Values.....	65
3.7 Summary of Radiation Calculation Parameters.....	68
3.8 Room Conduction Backlosses.....	75

LIST OF FIGURES

Figure	Page
2.1 Overall Room Plan View.....	19
2.2 Experimental Room Plan View.....	22
2.3 Experimental Room North Wall Elevation.....	23
2.4 Experimental Room East Wall Elevation.....	24
2.5 Heated Panel Assembly.....	25
2.6 Air Flow Measurement Box Elevation and Plan Views.....	29
2.7 Air Flow Measurement Box Nozzle Bank Layout.....	31
2.8 Typical Cross-section of Measurement Box Pressure Tap.....	32
2.9 Coil and Chiller Control Schematic.....	35
2.10 Room Inlet Temperature Thermocouple Arrangement.....	45
2.11 Room Inlet Temperature Gradient.....	46
3.1 Experimental Room Interior Elevation, Heated Panel Layout.....	52
3.2 Panel Temperature vs. Time - 100°F Setpoint, 820 & 165 cfm.....	53
3.3 Nozzle, Room Inlet, and Outlet Temperatures vs. Time (5 ach w/ foil).....	56
3.4 Nozzle, Room Inlet, and Outlet Temperatures vs. Time (5 ach).....	57

LIST OF FIGURES, CONTINUED

Figure	Page
3.5 Nozzle, Room Inlet, and Outlet Temperatures vs. Time (10 ach).....	58
3.6 Nozzle, Room Inlet, and Outlet Temperatures vs. Time (15 ach).....	59
3.7 Nozzle, Room Inlet, and Outlet Temperatures vs. Time (20 ach).....	60
3.8 Nozzle, Room Inlet, and Outlet Temperatures vs. Time (25 ach).....	61
3.9 Room Heat Balance - Air Heat Gain vs. Panel Power.....	65
3.10 Ceiling Temperature Versus Time	72
3.11 Modified Heat Balance - Energy Out vs. Energy In (5 ach).....	76

NOMENCLATURE

CFM	volumetric flow rate (ft^3/min)
ACH	air changes per hour
Q_{panels}	heat gain from panels (btu/hr)
Q_{air}	heat gain to air (btu/hr)
c_p	constant pressure heat capacity (btu/lbm- $^{\circ}\text{F}$)
β	nozzle beta ratio
β	thermal expansion coefficient ($^{\circ}\text{F}^{-1}$)
α	nozzle alpha ratio
α	thermal diffusivity, $k/\rho c_p$, (ft^2/hr)
ν	kinematic viscosity, μ/ρ , (ft^2/sec)
Y	expansion factor
C	nozzle discharge coefficient
g	gravitational acceleration ($32.2 \text{ ft}/\text{sec}^2$)
R	universal gas constant ($53.35 \text{ ft}\cdot\text{lb}/\text{lbm}\cdot^{\circ}\text{R}$)
p_e	saturated vapor pressure

NOMENCLATURE CONTINUED

ρ_p	partial vapor pressure
ρ_o	atmospheric air density (lbm/ft ³)
ρ_x	chamber air density at plane x (lbm/ft ³)
k	thermal conductivity (btu/°F-h-ft)
μ	viscosity coefficient (lbm/ft-sec)
E	energy factor
CWS	chilled water supply
CWR	chilled water return
e_i	experimental uncertainty of measurand I
J_i	radiosity of surface i (btu/hr-ft ²)
W_{bi}	blackbody radiation of surface i (btu/hr-ft ²)

CHAPTER ONE - INTRODUCTION

1.1 Background

An experimental heat transfer facility has been constructed at Oklahoma State University to study interior convective heat transfer in rooms. There are three primary heat transfer processes that occur within building structures: longwave radiation, conduction, and convection. Both conduction and radiation processes are reasonably well understood and can be modeled accurately in building simulation programs. Furthermore, current literature is relatively consistent when it comes to the prediction and modeling of these two heat transfer processes in buildings. In contrast, the literature covering both analytical and experimental studies of convective heat transfer show marked disagreement for many of the heat transfer situations encountered in buildings. In light of this, an experimental facility was designed and constructed to allow experimental investigation of interior convective heat transfer in rooms.

1.2 Literature Review

A summary of experimental studies (full size and scale models) mainly investigating forced convection in enclosures is given. Closely related, but not included in this review, would be a number of publications covering research into room airflows. See Ramey (1994) or Weathers (1992).

The main focus here is on full size and scale model studies aimed at investigating convection heat transfer in rooms for forced ventilation. A few

¹ Two forms of radiation impact building heat transfer: short-wave and longwave. Radiant exchange within the internal environment (longwave radiation) will be the focus here, versus solar radiation entering from the external environment (short-wave radiation).

natural convection experiments are covered also, mainly due to their focus on convection coefficient measurements. Akbari et al. (1986 and 1987) provides a good background for these studies. Akbari demonstrates analytically and numerically that an accurate characterization of the interior convection coefficient is critical to energy analysis in buildings, especially for buildings with thermally massive walls. As stated by Khalifa, of the three modes of heat transfer in buildings, longwave radiation, convection, and conduction, convection is the most complex. Additionally, Spitler et al. (1987) and Akbari et al. (1986 and 1987) both point out that recent construction practices have produced marked variations in convective heat flow paths. Weber (1980) adds to this that for most buildings undergoing normal operation, the interior surface convection coefficients will vary dramatically depending on the HVAC system mode of operation. Most importantly, even current "state-of-the-art" hourly analysis load programs and available literature utilize outmoded and inappropriate convection correlations. All of these factors point to the need for more thorough research and robust experimental studies to determine the contribution of convection in building heat transfer.

The following literature review is grouped according to investigative body and ordered alphabetically by principal investigator. A summary highlighting principle investigator, date of work, enclosure size, and working fluid is shown in Table 1.1.

Table 1.1 An Overview of Convective Heat Transfer Experiments

Principle Investigator	Date	Convection Flow Regime	Working Fluid	Dimensions LxWxH (ft)
Bauman	1982	natural	water	2.5 x 0.83 x 0.42
Bohn	1984	natural	water	1.0 x 1.0 x 1.0
Chandra	1984	natural & forced	water	17.7 x 11.7 x 8.1
Khalifa	1989	natural & forced	air	9.7 x 7.7 x 6.8
Neiswanger	1987	natural & forced	water	0.9 x 0.65 x 0.65
Spitler	1991	forced	air	15.0 x 9.0 x 9.0
Spitler	1987	forced	air	14.6 x 12.0 x 8.5
Weber	1980	natural	freon	4.7 x 2.4 x 1.4

1.2.1 Full Scale Facilities

Florida Solar Energy Center (FSEC)

(1984) *Chandra et. al.*

A full-scale room was constructed at the FSEC to investigate room airflows under both natural and forced convection conditions. The room is located on the southeast corner of the FSEC Passive Cooling Laboratory (PCL) and has dimensions 17'-8" x 11'-8" x 8'-1". The room has a slab-on-grade floor with rubber pad and carpeting. The walls are conventional stud frame insulated to R-11 for the two exterior walls and R-25 for the two interior walls. Wall interior surfaces consisted of unfinished gypsum board. The facility also consisted two windows on the east side with two wing walls to facilitate room air circulation.

The room was first heated using two 1350 watt heaters. A ceiling fan was allowed to run during this time. Next the heaters and fan were turned off for 15 minutes and removed from the room. The windows were then opened and the room was allowed to cool. Data was taken for two hours thereafter.

The west wall was constructed with an additional three heat transfer panels. Thermocouples were embedded in these panels and mounted on the remaining five surfaces and in the window openings. Measurements of velocity and temperature were taken every ten seconds and averaged over a five minute period.

Convection coefficients were isolated by performing a surface heat balance on the west wall surface. Furthermore this heat transfer data was correlated to local surface airspeeds and compared to ASHRAE values.

Solar Energy Unit, University of Wales

(1989) Khalifa et. al.

A full size test cell with dimensions 2.95m x 2.95m x 2.08m was constructed to study natural and forced convection on interior building surfaces. The test cell consisted of two separate zones, a large hot zone and a smaller cold zone. Both zones were controlled to different temperatures to obtain a temperature differential across the dividing partition. Hot zone dimensions were 2.95m x 2.35m x 2.08m. The cold zone had the same length and height but width of 0.6m. All four walls and the roof of the hot zone were constructed of 50mm thick isocyanurate board covered with aluminum foil on both sides. The floor of the hot zone was constructed of 100mm thick styrofoam board covered with a 19mm thick chipboard on both sides. All three walls, the roof and the floor of the cold zone were constructed of 3mm thick hardboard.

Facility instrumentation consisted of arrays of thermistors mounted through the two zones. These measured surface temperatures, as well as, adjacent air temperatures. The cold zone temperature was controlled by circulating ambient air via an extraction fan. The hot zone used a small fan heater to heat the zone. Both zones used proportional temperatures controllers.

The facility was allowed to reach a steady condition by allowing for a 24 hour run between any two different temperature settings. Each test produced

about 12 hours of temperature data which was read by a 60 channel datalogger and analyzed by a BASIC computer program.

Khalifa provides an expression for the calculation of the convective heat flux, as well as, the convective heat transfer coefficient. This is accomplished by letting the insulation slab form the heat flux meter. Thus in a steady-state condition the heat flowing from the air to the wall surface by convection should be equal to the heat loss by conduction through the wall.

Twenty-seven data points were correlated by multi-regression with the convection coefficient a function of temperature difference. Results of the correlation were compared to currently available correlations in existing literature. The results of these comparisons indicated that the convection coefficients resulting from real sized enclosures are considerably higher than those reported for isolated surface.

University of Illinois at Urbana-Champaign, UIUC

(1991) Spitler et. al.

A full scale heat transfer facility was constructed at the University of Illinois. This facility, which rested on the floor, made use of 53 individually controlled panels (static) to control the temperature of the room interior surfaces. A pattern control algorithm (Fisher 1989) was shown to provide significantly better panel temperature control than a simple set point or predictive control algorithm (Althof 1987). The panels were heated by way of nickel chromium resistance wires covered with plaster. Room surfaces were instrumented with

thermocouples and controlled to 86°F for all tests. One of the walls implemented plate coils to accommodate future cold wall instrumentation.

Tests performed included the following:

- Volumetric flow rate - 15, 30, 50, 70, and 100 air changes per hour.
- Inlet temperatures - 61°F, 70°F, and 79°F.
- Inlet locations - ceiling and side wall.

The airflow measurement system was based on ANSI/ASHRAE Standard 51-1985. Additionally, the facility implemented an air speed and air temperature measurement system.

Heat balance calculations were performed and were shown to be within the allowable uncertainty range. While the facility was constructed to accommodate various interior building heat transfer experiments, the primary focus of the work was interior convective heat transfer. Specifically, the convection coefficient was empirically calculated. The convective component of heat transfer was isolated as per the following equation:

$$q_{conv} = q_{in} - (q_{rad} + q_{cond}) \quad [1.1]$$

In the above equation, panel power input is known, the radiative contribution of each surface is calculated, and the conductive back-loss is shown to be negligible. The convection coefficient was then calculated according to the following equation:

$$h_{conv} = \frac{q_{conv}}{A_s(T_s - T_r)} \quad [1.2]$$

Emphasis was placed on the proper choice of the reference temperature.

Four different reference temperatures were investigated:

- room inlet
- bulk air temperature
- air temperature adjacent to surface
- air temperature as a function of height

An approximately linear relationship was shown to exist between the room outlet based film coefficients and the volumetric flow rates. Thus the room outlet temperature was chosen as the reference temperature.

A total of forty experiments were performed and a detailed uncertainty analysis due to measurement of temperature, panel power, and volumetric flow rate was also presented. Results were obtained from this facility for thirty-seven high ventilative flow rate experiments. A heat balance, energy in to panels versus energy gained by the air, was calculated for all thirty-seven cases. These heat balance results showed that actual room performance was better than the conservative error estimate that was presented.

A correlation between the convective film coefficients and the jet momentum number (J) was developed. This correlation was used to develop a new convective heat transfer model for various air supply inlet and ranges of J .

The correlations were based on two observations that followed from the experimental results:

1. h_c was linearly proportional to the bulk air velocity.
2. Bulk air velocity is proportional to the square root of the jet momentum.

This new model is contrasted with the natural convection model currently used in building design and simulation programs. These two models were implemented in the Buildings Loads Analysis and System Thermodynamics (BLAST) program and an office building was simulated using the two models with significantly different results.

(1987) *Spitler et al.*

An enclosure with modeled interior and exterior environments was constructed. Two sides of a 4.5m x 3.6m x 2.6m room were adjacent to a temperature controlled airspace and the other two sides were adjacent to a space in which the temperature was allowed to float. The walls were 20.3 cm thick and the two heated surfaces were instrumented with heat flux transducers.

The facility made use of a window-type air-conditioner and reheat coils connected to a standard air distribution system for room air temperature control. The room utilized a centered ceiling diffuser inlet air configuration. This was the only air inlet configuration investigated. A sol-air space was heated via electric resistance heaters and fans. The facility, which rested on the lab floor, measured surface temperature, room air temperature, and cooling system air temperature, as well as, surface heat flux.

The convection coefficient was isolated by subtracting the radiative flux from the total flux. This local film coefficient was found to have strong dependencies in the vertical direction. Also, a strong correlation was seen to exist between a heat exchanger effectiveness model and mass flow and temperature difference.

The study stressed the need to accurately measure the convective and radiative portions of building heat transfer. Attention was brought to the fact that previous studies have not sufficiently addressed the dynamics of flow in full scale enclosures, nor have they been responsive to the significant changes in convective patterns due to recent construction trends.

1.2.2 Scale Models

Lawrence Berkeley Laboratory (LBL), University of California
(1980) Bauman et. al.

A large body of work conducted at LBL has been devoted to natural and forced convection heat transfer analysis in buildings. One such group of experiments investigated buoyancy-driven convection in rectangular enclosures. The flow regimes investigated within these enclosures was meant to be representative of many passive solar systems.

The natural convection experiment made use of two scaled models: one single zone and one two room zone with a partition. Water was used as the working fluid. The rectangular apparatus had dimensions 12.7cm x 25.4cm x 76.2cm fabricated of 1.3cm clear plexiglas. The two 76.2cm side walls were

sufficiently long enough to create the two-dimensional problem and were fabricated with cold rolled copper sheets. The hot wall was energized using six thermofoil heaters mounted on the outside surface of the copper plate. The cold wall was constructed with copper tubing mounted on the copper plate surface. Cold tap water was circulated through the copper tubing.

Thermocouple probes were arranged to measure vertical temperature gradients within the fluid. Also thermocouples were embedded within the copper plates of both the hot and cold plates. The heaters and water flow rates were set to the desired levels and the entire system was allowed to reach equilibrium (about 3-4 hours). Thermocouple readings were taken over a period of about 15 minutes. The heat input rate was measured using a wattmeter. Heat output rate was determined by measuring the cooling water inlet-to-outlet temperature difference and by calculating the cooling water volumetric flow rate.

For each experiment, average plate temperatures were calculated and used to evaluate the characteristic Rayleigh number. Heat input and output values were used to find average Nusselt numbers for the hot and cold plates.

Solar Energy Research Institute (SERI)

(1983) Bohn et. al.

A cubical enclosure was constructed to study three-dimensional natural convection at high Rayleigh numbers ($Ra \approx 10^{10}$). Water was used as the working fluid with all four walls having the capacity to be heated or cooled. The top and bottom were transparent and considered adiabatic.

The test cell had cubical dimensions of 30.5cm and consisted of eight 1.27cm thick aluminum plates. Four inner plates form the actual enclosure with the four outer plates providing for the heating and cooling of the enclosure walls. Three of the walls had thermocouples centered and within 3mm of the inner surface. The fourth wall had eight thermocouples placed in such a way to measure wall spatial temperature variations. These variations were less than 5% of the overall wall temperature difference, $T_h - T_c$. Thus the walls were considered to be isothermal. For flow visualization purposes 1.27cm thick Lucite plates were attached to the test cell top and bottom. The four walls were insulated with 8.3cm thick foam board insulation.

Heat loss from the insulated walls was estimated to be 0.1% of the total wall heat loss. The top and bottom plates were considered adiabatic and the end conduction for overlapping plates was estimated to be about 0.8%.

Cooling and heating of the four cell walls was accomplished by circulating hot or chilled water through milled channels in the outer plates. Heat was supplied to the water via a 6kw in-line electric heater in combination with a domestic hot water tank. A proportional temperature controller controlled leaving tank temperature to within ± 0.25 °C. Cold tap water was also circulated through the channels and controlled to within ± 0.25 °C. Rotameters measured cooling and heating flow rates.

An approximate error analysis yielded experimental convective heat transfer accuracy to within $\pm 5.0\%$ of actual values.

Water properties were calculated at a temperature equal to the four wall average, denoted as the bulk temperature. Rayleigh number was calculated based on the hot to cold wall temperature difference and the Nusselt number was calculated based on the bulk to wall temperature. The characteristic length used for both the Nusselt and Rayleigh numbers was 30.5cm.

For each experimental configuration a 24 hour runtime period was required to reach a steady state condition. Hot to cold wall temperature difference was taken as the measuring value for steady state conditions.

A total of four wall heating/cooling configurations were investigated and several different ranges of Rayleigh numbers were calculated. Tests revealed an inactive core surrounded by boundary layers on each of the four vertical walls. Heat transfer measurements consisted of average heat transfer coefficients for each wall. Data was plotted for Ra vs. Nu on a log-log plot and revealed a straight line relationship. For heat transfer coefficients based on wall to bulk temperature difference a single correlation was developed that agreed well with analysis and two-dimensional enclosure flow. The correlation indicated that a laminar boundary layer flow heat transfer mechanism exists even at the higher Rayleigh numbers.

University of California

(1987) Neiswanger et. al.

A small-scale test apparatus with uniformly heated walls and adiabatic top and bottom was constructed to study high Rayleigh number mixed convection. The rectangular enclosure has dimensions interior dimensions 20cm x 20cm x

27.4cm. The top and bottom sections were made of 12mm thick transparent acrylic plastic as were the end walls. Water was used as the working fluid and heat transfer through the plastic was negligible. Two full height and 1/3 width openings on both ends allowed flow to pass through the test section. For the longer side walls .0264mm thick Iconel foil was stretched over a 25.4mm thick layer of polystyrene foam insulation. The water flow system consisted of a 246 liter storage tank, a pump, a rotameter and PVC distribution lines. Electric power to the foil was supplied by an 1800 watt dc power supply.

Thermocouples were mounted on the two side walls and at the test section entrance. After power was set for the foil heaters and pump the system was allowed to equilibrate for about 15 minutes. Local and mean heat transfer coefficients were determined for the wall surfaces. Neiswanger does not describe how these coefficients were calculated. Also, a mixed convection heat transfer correlation was developed and compared favorably with the experimental data.

University of Idaho

(1980) Weber

Weber reported on an experimental study of natural convection heat transfer through a doorway in a two room passively heated building. Similitude modeling was used to measure the natural convection heat transfer coefficients with freon being used as the working fluid.

The prototype to be modeled, which was not actually constructed, was a simple two room arrangement with the following components: a separating

partition with doorway, a trombe wall on one end, and a thermal storage wall on the other end. The dimensions were 24' x 12' x 7'.

For the 1/5th scale model, a 1" polystyrene partition with an aperture (doorway) separated the two rooms. A temperature difference between the two rooms was maintained by a heated vertical wall at one end and cooled vertical wall on the other. Overall scale dimensions were 56" x 29" x 17". The cold wall consisted of two plates, one aluminum and one copper, separated by an air gap. Copper tubing, for coolant water circulation, was mounted on the inside surface of copper plate. Thermocouples were mounted in the vertical direction at the cold plate center. The hot wall consisted of a copper and aluminum plate separated by an air gap followed by a heating element, which was enclosed in a polyurethane enclosure to reduce back losses. The heating element consisted of nichrome wire suspended one inch behind the copper plate.

The air-tight scale model was filled with freon and, with the cold and hot walls at steady state, temperature measurements were made. A total of 80 thermocouples were mounted throughout the model to measure gas temperature, external wall temperatures and cold and hot wall temperatures.

Natural convection heat flow through the aperture was calculated by subtracting the hot cell heat losses from the hot plate power input. This heat transfer through the doorway was measure as a function of the average temperature differential between the two rooms and the geometry of the aperture.

The natural convection coefficient and average temperature difference were expressed in terms of Nusselt, Grashof and Prandtl numbers. Two ratios: door height to ceiling height (AHR) and door width to partition width (AWR) were investigated for natural convection dependence.

1.3 Objectives

The main objective of this work is to design and construct an experimental facility to study convective heat transfer in rooms. The room design is intended to be an improvement upon the design of a previous facility constructed at the University of Illinois at Urbana-Champaign (UIUC). Significant improvements include the following:

- Design implements a grid of 2' x 4' removable panels which may be heated or cooled or replaced with an inlet or outlet²
- Experimental room has been elevated approximately five feet off the lab floor. This allows for the environmental control of the space surrounding all six surfaces and reduces the heat loss by conduction through the floor.
- Experimental room is larger offering more flexibility
- Air measurement system has been designed to allow for finer measurement of volumetric flow rates ranging from 160 to 3500 cfm.
- A 250 gallon chilled water tank has been coupled with a water-to-water heat pump allowing for a more uniform and constant supply of chilled water to the fan/coil unit. This increases the ability to provide a constant inlet temperature to the room.

²For the purposes of this study, the term "room inlet" shall be taken as the room air supply opening.

The facility, still in initial testing stages, also has many potential uses for further study and investigation. While the initial shakedown tests will be aimed at investigating overall facility performance, more detailed studies are anticipated. For instance, the experimental room data could be used to validate CFD models of room air flow. Also, convective heat transfer from common office equipment, lights in plenums, and windows might be considered. Lastly, the versatile nature of this facility lends itself to the study of most heat transfer processes occurring in buildings today. To these ends, this study seeks to provide a basis for further investigation by validating the current facility performance through experimental tests and providing sufficient information on the background and design of such facilities.

Focus here will be on the air system side design and construction, as well as room air flow measurement and facility heat balance performance. A complementary thesis, Sanders (1995), focuses on heated panel control and overall experimental room construction.

CHAPTER TWO - EXPERIMENTAL FACILITY

2.1 Overview of Experimental Facility

The experimental room can best be described as an isolated, honeycomb-like structure with well insulated walls. The floor of the facility is located approximately 30 feet below grade. This below grade condition makes the facility less susceptible to external variations in temperature. Overall laboratory dimensions are 37.5' x 30' x 20'. A guard space³, made up of 2x4 studs and R-11 insulation surrounds the actual room and has dimensions, 28' x 20.5' x 20'. The only connections the laboratory had with the external environment were the supply and return grilles from the building HVAC system. Effects this may have had on facility performance were deemed minimal enough to neglect. Figure 2.1 shows an overall facility layout and the following sections will discuss various room features pertinent to the initial validation tests. Flex ducting shown in Figure 2.1 indicates the current inlet/outlet configuration.

³ The walls of the guard space have not been completed yet.

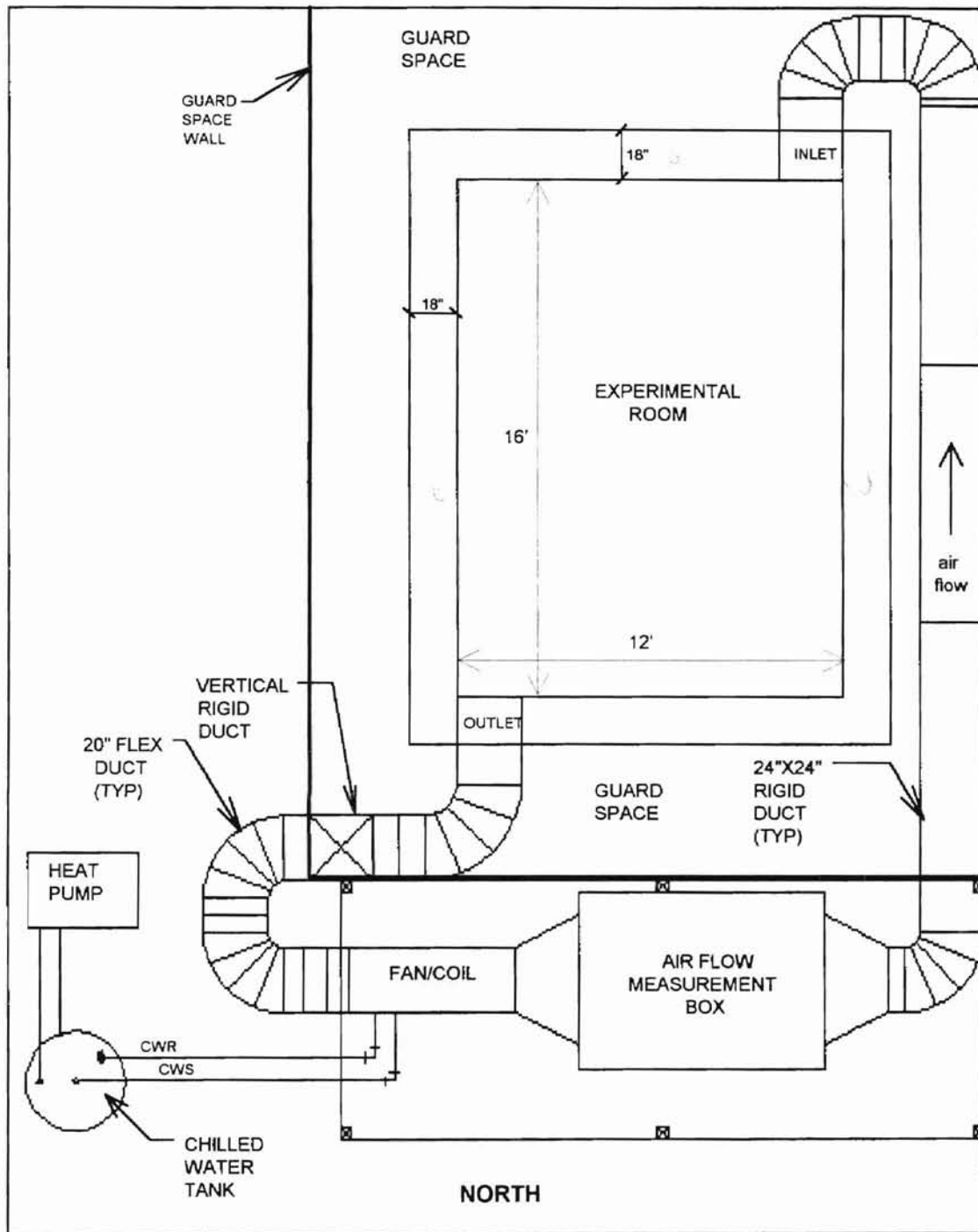


FIGURE 2.1 Overall Room Plan View

2.2 Room Description

The experimental room has interior dimensions 12' wide by 16' long by 10' high and is elevated 5' off the laboratory floor. The walls consist of two 2" x 4" stud walls, with spacers installed to give an overall wall thickness of 18". Using dado cut lap joints and epoxy, the wall members are partitioned off in a 2' x 4' grid. This arrangement forms the 2' x 4' x 1.5' cells. The walls of each cell are lined with 1/4" masonite and all voids are filled with cut-to-fit insulating styrofoam bead board. The wall cells are then filled with insulation pillows consisting of four layers of R-19 insulation wrapped in plastic. The back of each cell is covered with a removable 2' x 4' section of 1/2" plywood. The front of each cell (room interior) provides for the mounting of the 2' x 4', removable heated panels. These panels will be discussed further, later in this section. The overall thermal resistance value for the wall assembly is approximately R-67.

The floor and ceiling were constructed using two layers of 2"x8" studs to give an overall nominal thickness of 16". They also were partitioned off in a 2' x 4' grid to form the cells. These cells were filled with the insulation pillows (3 layers of R-19) also and backed with 1/2" plywood. The floor and ceiling inside faces also allow for the mounting of the removable heated panels. The overall thermal resistance value for the floor/ceiling assembly is approximately R-47.

The 18" thick walls and 15" thick floor/ceiling form a channel at the room perimeter. This channel was framed with 1/2" plywood and filled with R-19 insulation. Figures 2.2 - 2.4 show typical room elevations and plan views for clarity. Also, room interior thermocouple placement is shown in Figure D.1 of

Appendix D. Sanders (1995), gives additional information regarding overall room construction.

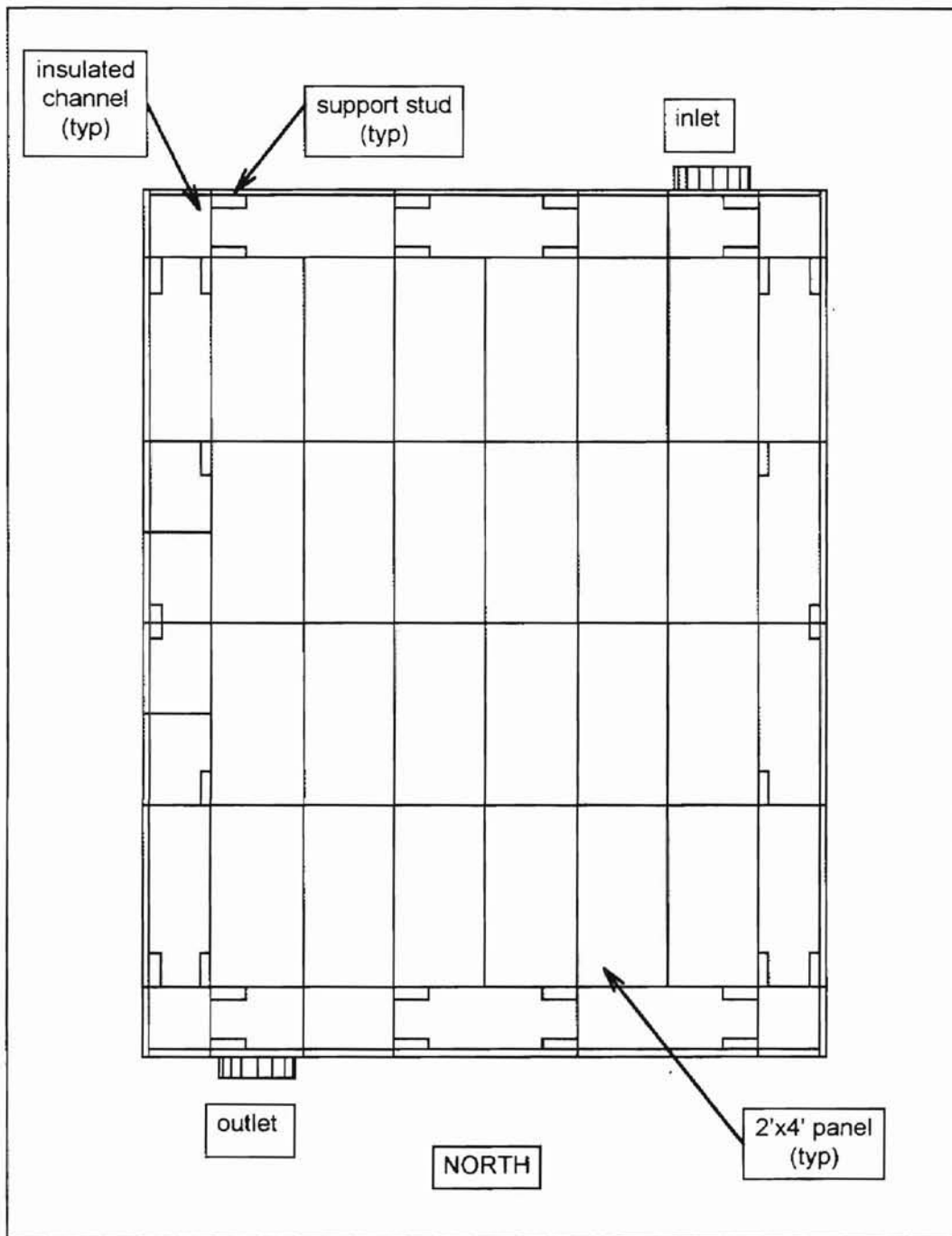


FIGURE 2.2 Experimental Room Plan View

OK

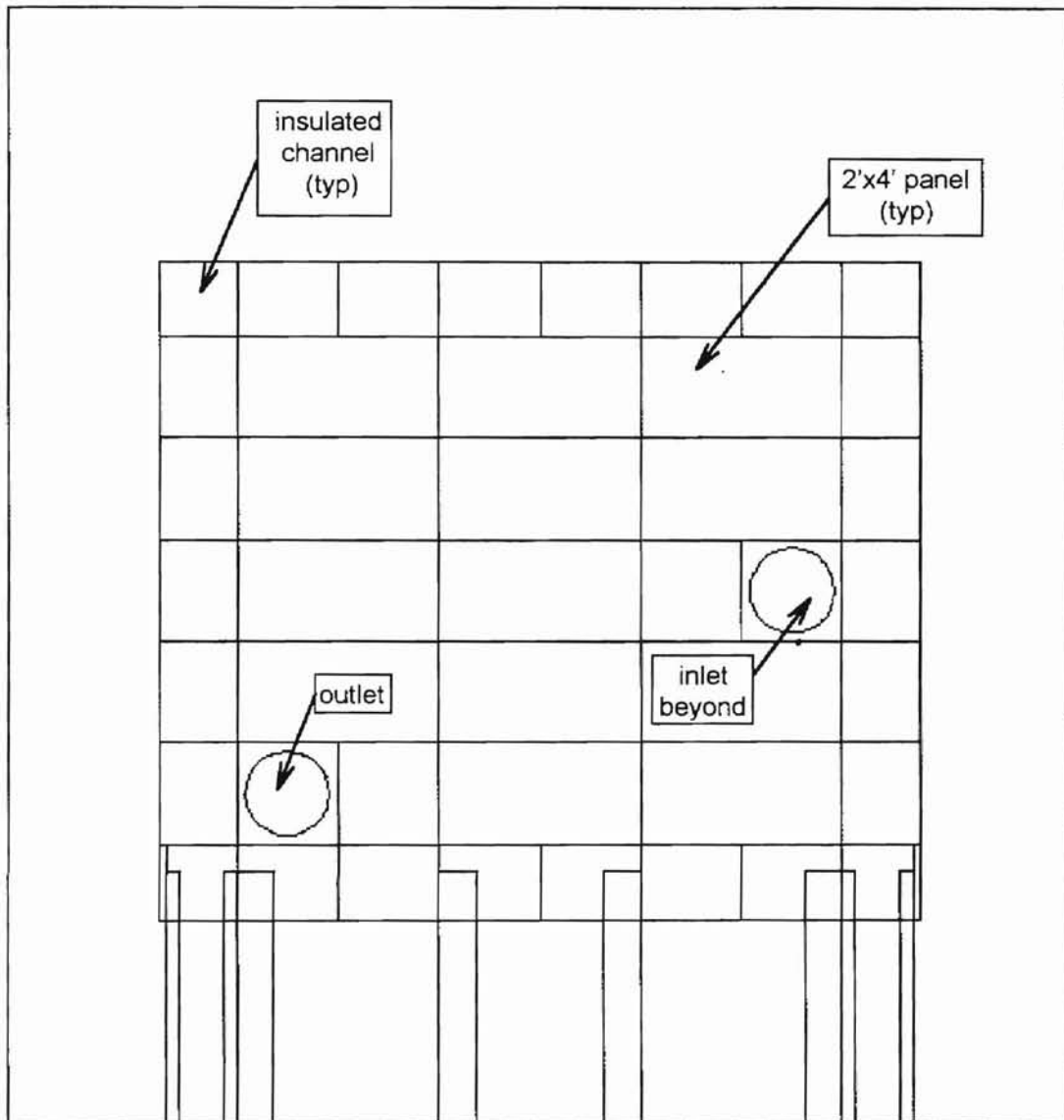


FIGURE 2.3 Experimental Room North Wall Elevation

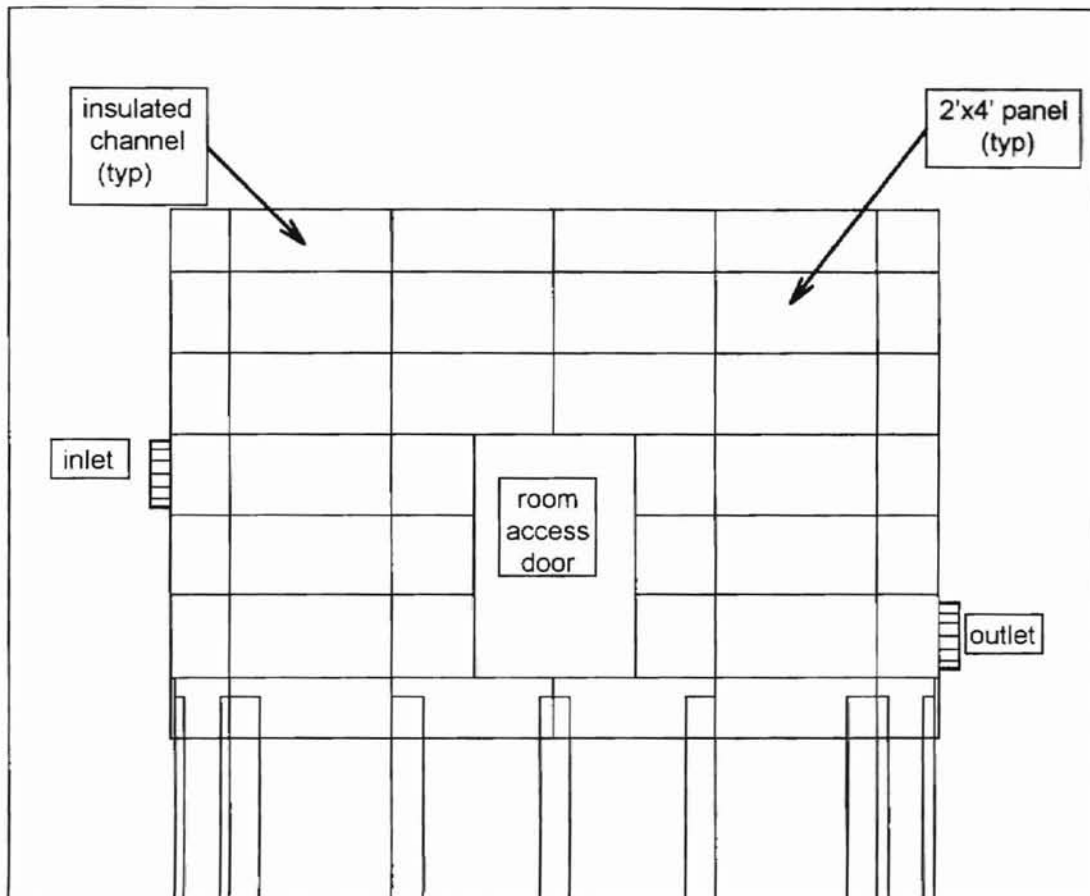


FIGURE 2.4 Experimental Room East Wall Elevation

2.2.1 Modular Heated Panel System

The 2' x 4' panels consisted of nickel-chromium wire affixed to the surface of 5/8" gypsum board. This wire was then covered with a 1/2" layer of gypsum plaster. A conduction analysis program was written to determine proper spacing between wire rows (Sanders, 1995). A Type T thermocouple was embedded in plaster near the panel surface for panel temperature measurement. A panel cross-section is shown in Figure 2.5.

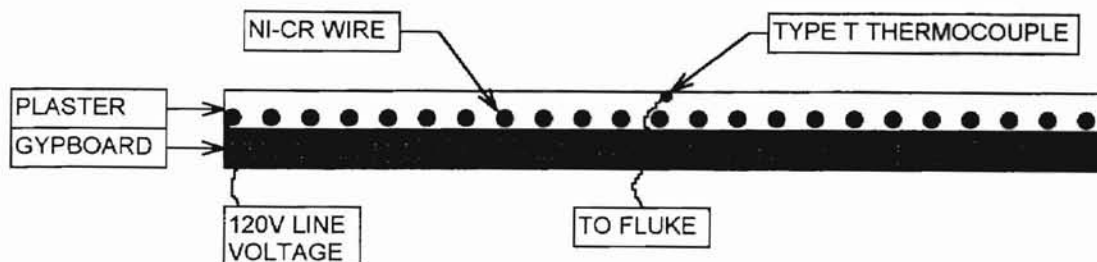


FIGURE 2.5 Heated Panel Assembly.

2.2.2 Room Instrumentation and Controls

Currently, twelve heated panels have been installed, all on the west wall. The other surfaces are currently passive surfaces. The heated panel system requires a control scheme to maintain panel surface temperatures at desired levels. This is accomplished using a "pattern" control algorithm which is described by Fisher (1989) and Sanders (1995). This algorithm is implemented in a BASIC computer program, and controls the panels and samples room inlet/outlet and surface temperatures. Twelve Type T thermocouples (one per panel) are placed near the surface of each panel and are connected to a Helios Fluke Datalogger. The Fluke samples panel temperatures approximately every 5 seconds. The electromotive force voltage (emf) of each thermocouple is read and passed on to the Fluke datalogger to determine respective temperatures. The temperatures are then passed on to the serial port of the lab IBM cpu. The control algorithm, which is fully described in Fisher (1989) and Sanders (1995), returns control bytes to the digital I/O board. The digital I/O converts the control bytes into either a high signal ($\cong 5$ volts) or a low signal (0 volts). This signal is

then passed to a bank of solid state relays at the experimental room. These solid state relays are circuited to receive both a low control voltage signal (5 volts) and a 120 volt line voltage. On a high signal the solid state relay closes and 120 volts are passed to the panel's resistive wire circuit. On a low signal the solid state relay opens, short-circuiting the connection, turning the heated panel off. Additionally, twelve thermocouples were mounted on the passive walls, floor and ceiling.

2.3 Air System Description

The air system consists of a fan coil unit, an airflow measurement box, a reheat section and insulated ducting. The air system provides a known volumetric flow rate of conditioned air to the room and is described in detail below. An overall schematic is shown in Figure 2.1.

2.3.1 Fan Coil Unit

A fan-coil unit, mounted on the experimental room platform (Ref. Figure 2.1), utilizes a chilled water coil to provide conditioned air to the experimental room. The fan-coil unit was a Westinghouse 4 ton unit and part of a residential direct-expansion split system. The unit was converted to a chilled water fan-coil unit for the study at hand. The fan-coil unit was rated at 1600 cfm at 0.75" inches of water static pressure. The unit was converted to a chilled water fan-coil unit for the study at hand. The direct expansion coil header was removed and replaced with a chilled water header thus creating a chilled water coil. The fan-coil unit with a 3/4 horsepower fan motor, also contained a 10 KW resistance

heating coil. The resistance coil assembly was removed and retrofitted for installation as a reheat coil in the supply ductwork downstream of the air measurement box.

A variable voltage AC controller was used for most of the experiments to provide flow control of the supply air to the room. Spitler et. al. (1991) used flow control dampers placed in the return ducting. A combination of both fan control and damper control is suggested for future experiments to ensure proper control and inlet conditions at the air-flow measurement chamber.

Since the fan-coil unit was salvaged, a few performance indicators might be of interest. The fan-coil unit cooling capacities for the 5, 10, 15, 20, and 25 ach experiments are provided in Table 2.1. For these experiments the chilled water entering temperature ranged from 40–43 °F, subject to chiller cycling effect. Additionally, the fan-coil capacity is a function of the heated panel output. As such, the fan-coil entering and exiting air temperatures fluctuate with panel power fluctuations.

Table 2.1 Fan-coil Unit Performance

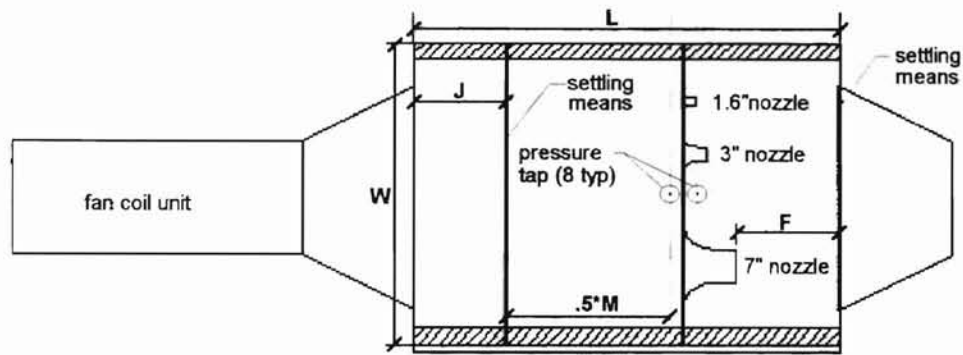
Experiment	Volumetric Flow Rate	Sensible Cooling (btu/hr)	Entering Air Temperature (°F)	Exiting Air Temperature (°F)
E091795C	5 ach (160 cfm)	3760	72.03	50.26
E091795A	10 ach (325 cfm)	6730	67.18	48.00
E091795B	15 ach (480 cfm)	7285	62.33	48.28
E091696	20 ach (650 cfm)	8285	60.85	49.05
E090995	25 ach (820 cfm)	8175	58.49	49.26

2.3.2 Air Flow Measurement Box

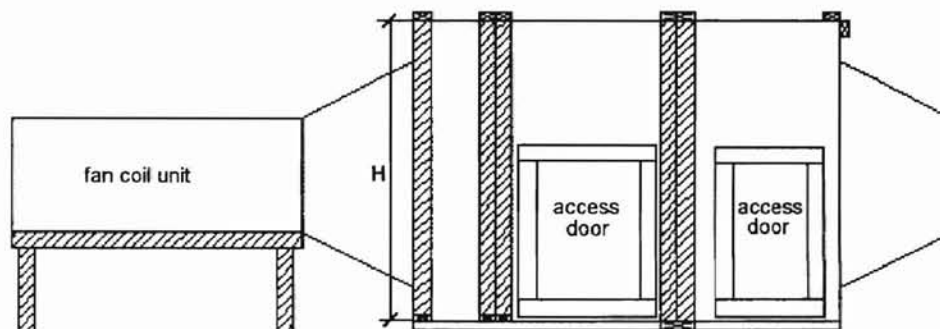
To obtain a meaningful heat balance, accurate measurement of the room supply air volume is necessary. To this end, an air flow measurement box was constructed. The basic design of the box is described by ASHRAE Standard 51-1985. This system utilizes the measurement of a pressure differential across a flow nozzle of known geometry (parabolic in this case) to calculate volumetric flow rate. This pressure differential occurs due to the sudden reduction in nozzle cross-sectional area. Further, the flow rate is proportional to the square of the resulting pressure differential. By applying the Bernoulli equation and the continuity equation, a theoretical formulation for volumetric flow rate is obtained. Further development of the equation allows for flow losses, jet contraction and compressible fluid flow effects. The equations used for this study are given in Appendix B.

The measurement box, constructed mostly of 2x4 studs and 1/2" plywood, is insulated with R-11 fiberglass batt to minimize heat loss. All joints are caulked and adhesive stripping has been applied to each access door to minimize air leakage. The construction is an "outlet chamber" set-up in accordance with ASHRAE Standard 51-1985. Elevation and plan views of the measurement box can be seen in Figure 2.6.

5 6



Measurement Box Plan View



Measurement Box Elevation

Figure 2.6 Air Flow Measurement Box Elevation and Plan Views.

A few measurement box design parameters, critical to ASHRAE Standard 51 should be mentioned. Referring to Figure 2.6, the following critical dimensions apply: $J = 17.0"$, $F = 22.0"$, $L = 110"$, $W = 63"$, $H = 64.5"$, and $M = 71.9"$. The dimension M is an equivalent diameter based on $H \times W$. Additionally, an equivalent diameter is calculated based on fan discharge dimensions, $A = 11.5"$ and $B = 13.0"$. This equivalent fan discharge diameter, D is used in the following

equation: $J = 1.2 \cdot D$. The ASHRAE Standard calls for a minimum of two settling means. The settling means were constructed of a fine grid hardware cloth installed across the cross-section of the measurement box. The standard allows for multiple layers of settling means for proper flow and backpressure requirements. However, this study utilized a single layer settling means for both the upstream and downstream conditions. The upstream settling means provide a uniform flow at the entrance to the nozzles, while the downstream settling means allow for proper back-pressure. Both conditions are critical for the measurement of the pressure drop across the nozzle bank.

For the initial testing, 7", 3" and 1.6" flow nozzles were installed in the measurement box. The overall measurement box is designed for the nozzle arrangement shown in Figure 2.7. The solidly outlined nozzles indicate those currently installed. At a design pressure drop of 0.8 inches of water across the nozzle bank, this gives minimum and maximum cfm limits of 18.6 (0.5 ach) and 3550 (110 ach) respectively. This will allow for a large range of experiments to be performed in the future. However, due to financial constraints we were unable to utilize the full capacity of this design. With the current design, we were able to produce flow rates ranging between 161 cfm (5 ach) and 820 cfm (25 ach) at 0.8" of pressure drop. Current nozzle layout accounts for edge effects as per the standard. Figure 2.7 shows the proposed future design and current nozzle layout. Refer to Appendix B for equations and calculations relating to air flow rate measurement.

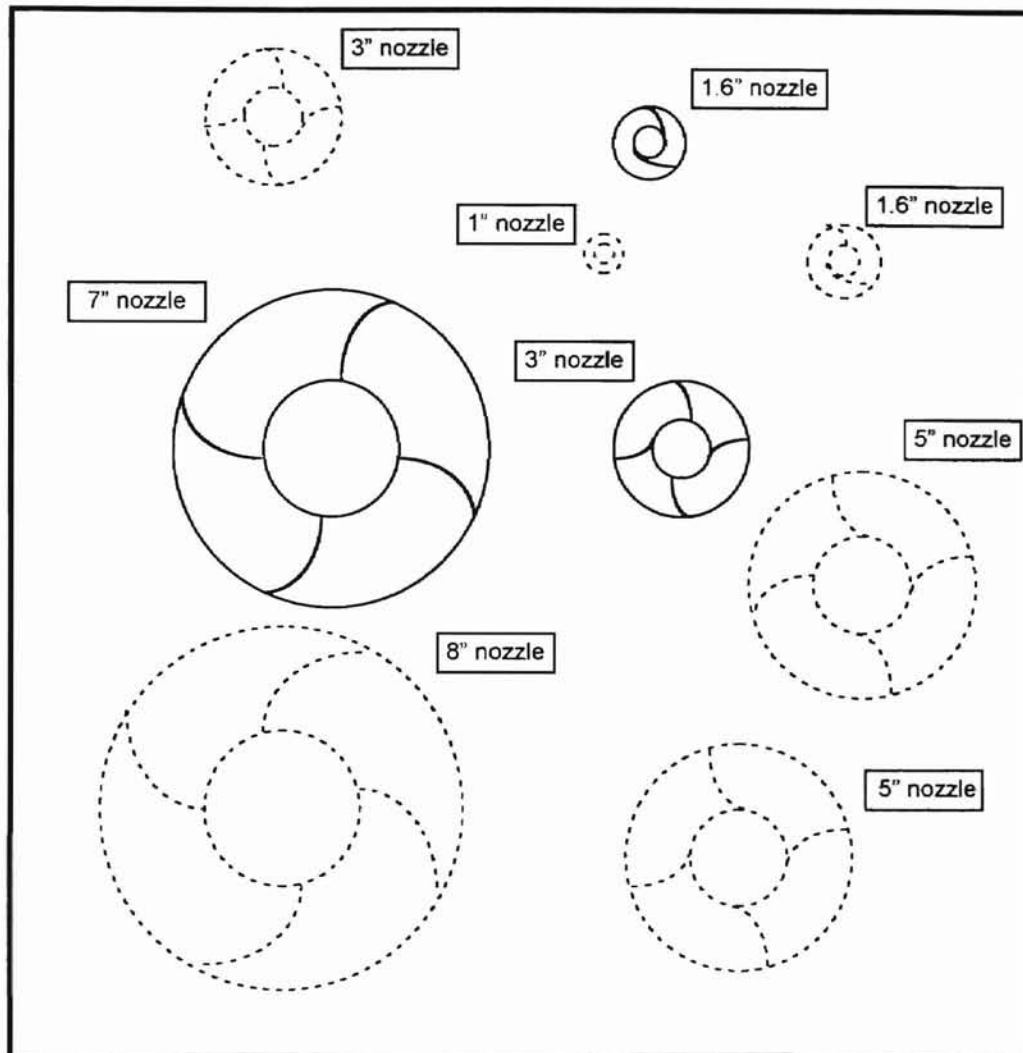


Figure 2.7 Air Flow Measurement Box Nozzle Bank Layout.

A total of 8 pressure taps were installed across the nozzle bank (four upstream and four downstream). Planes 5 & 6, of Figure 2.6, denote the center-line of the pressure taps on each side of the nozzle bank. This center-line is 1.5" \pm 0.25" from center of the nozzle bank. The pressure taps were mounted flush and connected to pressure averaging manifolds using 1/4" plastic tubing. This tubing was then connected to an inclined manometer for manual pressure

differential readings, in inches of water, across the nozzle bank. A detail of the pressure tap design is shown in Figure 2.8.

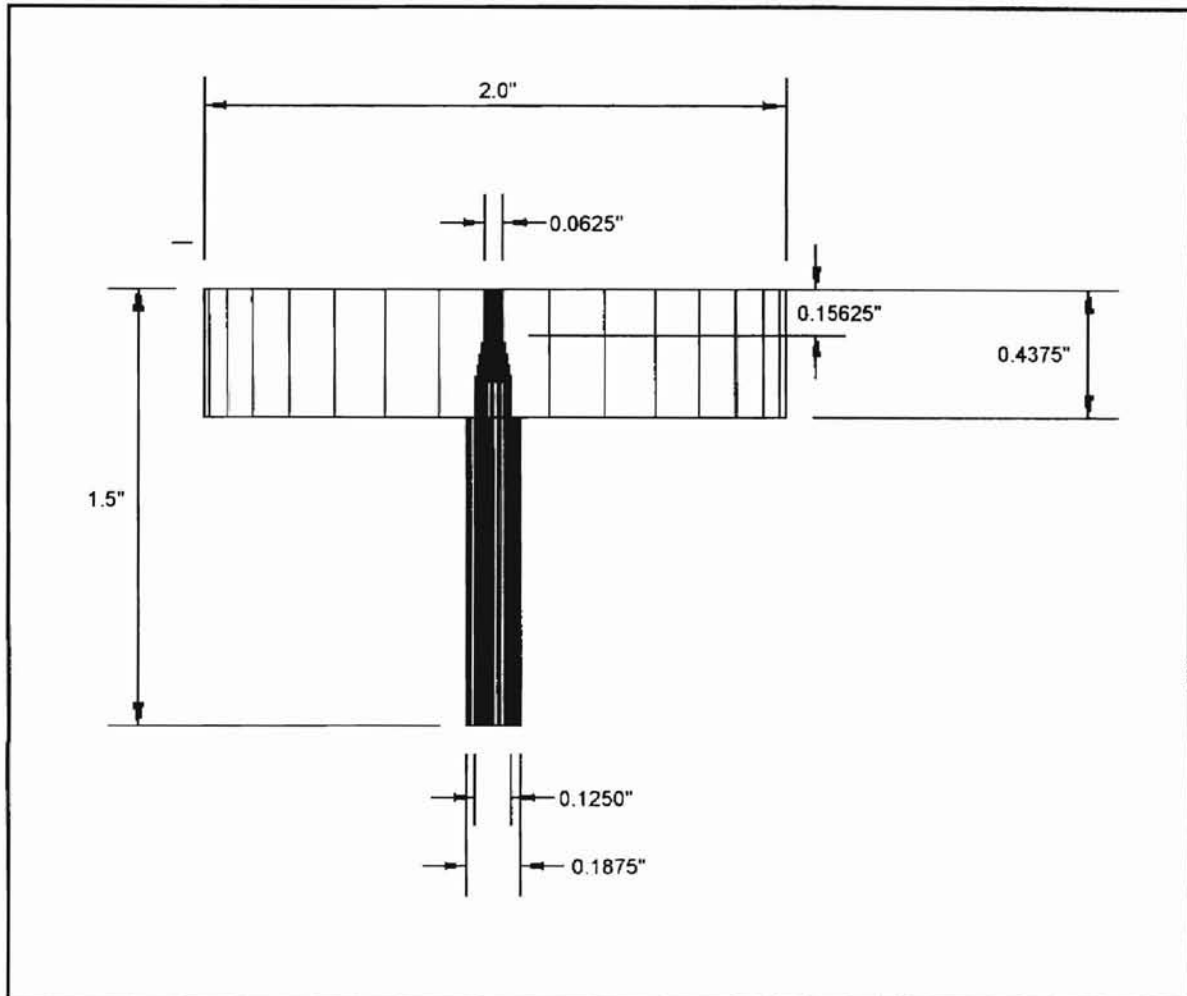


Figure 2.8 Typical Cross-section of Measurement Box Pressure Tap

2.3.3 Reheat Coil

A reheat section, for temperature control, was mounted in the duct just downstream of the measurement box. This reheat section was not implemented for the initial testing. Room supply temperature was a steady-state value limited

only by the set point of the water-source heat pump (i.e., room inlet was usually between 50 and 55 degrees Fahrenheit).

The reheat section, while not in working order at the time of the validation tests, will provide approximately 5kw of electric resistance reheat capacity. This will give much better room temperature control on future experiments and will allow the investigation of variable inlet temperature experiments. A companion project (Ferguson, 1991) investigated control of the resistance coils, using a proportional control algorithm in conjunction with solid state relays, and determined that reasonable control could be maintained with minimal overshoot and reasonable response time.

2.3.4 Ducting

The ducting system for the facility is quite basic and has the following components: Starting at the outlet of the measurement box, a 20" diameter flexi-duct section is connected to a 2' reheat section followed by 24 feet of 24" x 24" plywood duct. Another section of 20" flexi-duct is then connected to the south room inlet. At the north room outlet a section of 20" flexi-duct is connected to an 8 foot section of vertical plywood duct followed by a 20" diameter flexi-duct section which is then connected to the fan/coil unit at the air measurement box inlet. The general layout is shown in Figure 1.1. Each flexi-duct section has been designed with fittings that can be moved and adapted for a number of room inlet and outlet configurations. The entire air supply system is insulated and sealed to minimize heat loss and air leakage.

2.4. Chilled Water System

A constant flow of conditioned air was supplied to the room, via a chilled water system, utilizing a five ton water-source heat pump. Tap water was circulated through the heat sink heat exchanger (condenser) and the five ton chiller was set to a 40 degree Fahrenheit chilled water supply temperature. Chilled water was then supplied to a 225 gallon chilled water tank, using a small Grundfos circulating pump. This chilled water is discharged into the tank near the bottom in the vicinity of the coil loop outlet. A schematic of both the chiller and coil loops is shown in Figure 2.9. Water is supplied at the base and returned at the top of the chilled water tank to create a thermal gradient. This gradient allows for a constant temperature supply of chilled water to the fan/coil unit. Water flow rates were maintained between 4 and 6 gallons per minute. Also, both loops were supplied with manual regulating valves to allow for control of the coil temperature.

2.4.1 Chiller Controls

A chiller control box was also implemented to provide proper temperature control of the water-source heat pump, prevent damage to the chiller due to a dry heat exchanger, and cycle the chiller pump and waste water off when no cooling was required. A Goldline remote temperature sensing thermostat was used to measure chilled water tank temperature. Initially, short-cycling of the water-source heat pump was problematic and an improved control circuit was used. One problem was too tight of a floating temperature range (< 2 degrees F). This was adjusted to around 5 degrees Fahrenheit and chiller setpoint was set at

approximately 40 degrees Fahrenheit. A solenoid valve was connected to the chiller control switch. This valve, which shut off the condenser water when the chiller shut off, also required a shock control device to prevent damage to the piping design during sudden closing of the water valve. As a separate control, the coil pump switch was also included in the chiller control box. This separate circuit allowed for continuous circulation of chilled water to the fan/coil unit during the course of the experiments. A schematic shown in Figure 2.9 outlines the chilled water system and its controls setup.

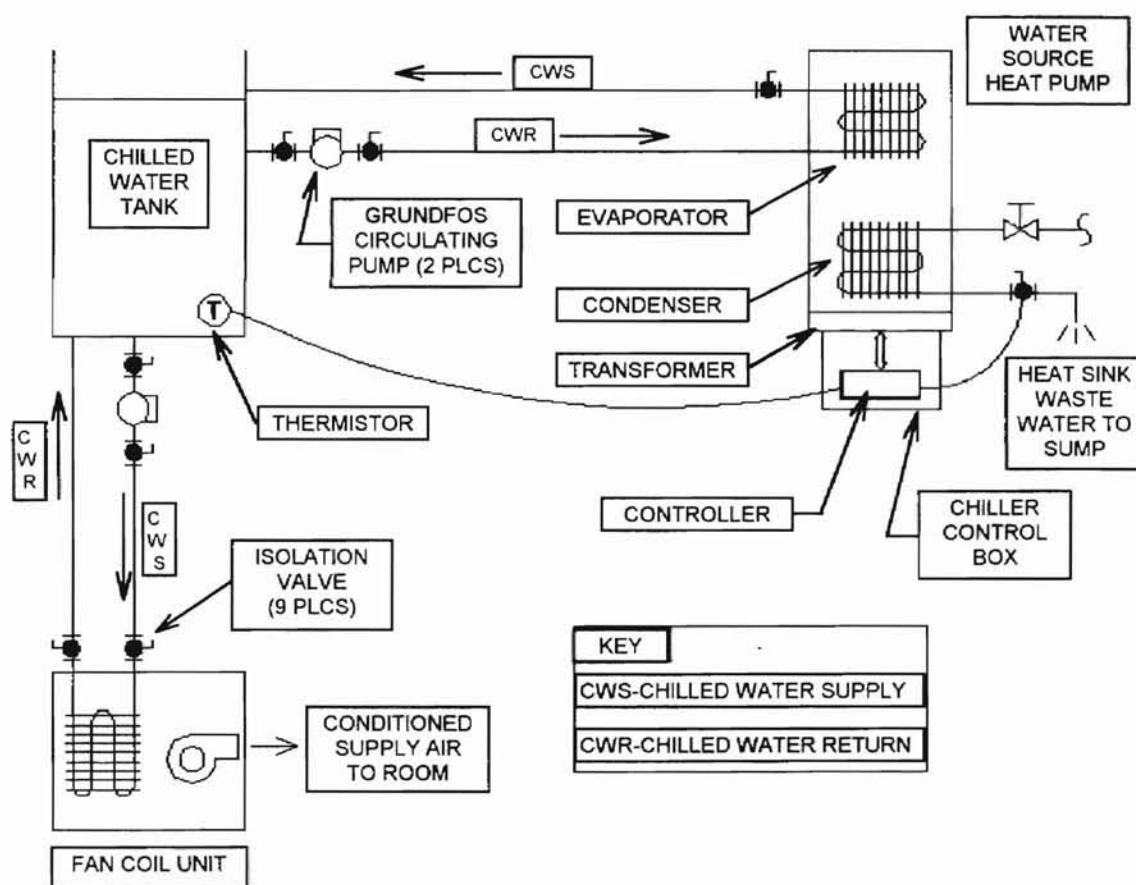


Figure 2.9 Coil and Chiller Control Schematic.

2.5 Air-Side Instrumentation

In addition to four thermocouples at the entrance of the airflow measurement box, four thermocouples were mounted at both the room inlet and outlet. Thermocouple readings were averaged to obtain room inlet and outlet temperatures. These spatial averages were susceptible to stratification at lower flow rates. The resulting uncertainties will be discussed later in section 2.8.

2.6 Data Acquisition

Each sampling by the Fluke datalogger is written to a data file for further processing. Depending on the length of each experiment this data file may be as large as 4 megabytes of temperature data. The BASIC computer program written to control the panels also retrieves the room inlet/outlet and surface temperatures. For each experiment large amounts of temperature and auxiliary data are generated. The auxiliary file contains the following echoed inputs:

- Desired panel setpoint ($^{\circ}\text{F}$)
- Experimental code
- Static pressure (inches of H_2O)
- Differential pressure (inches of H_2O)
- Barometric pressure (inches of Mercury)
- Drybulb and wetbulb temperatures ($^{\circ}\text{F}$)
- Current flow nozzle arrangement

It should be noted that most of this data was passed on to a separate data analysis program. This data analysis program and its functions will be explained later in chapter 3 and the source code can be found in Appendix A.

The temperature data file contained all passive surface temperatures, all twelve heated panel temperatures, the nozzle temperature and the room inlet and outlet temperatures for each sample, approximately every 10 seconds. Additionally, for each sample temperature data the program provided a counter, the fluke datalogger control text, and the twelve panel control bytes used in the analysis program to calculate panel power.

2.7. Experimental Procedure

Various experimental strategies were investigated and will be outlined here. Additionally, Table 2.1 shows a typical experimental observation log for three experiments.

While the chilled water tank, with its 225 gallons of capacity, provided excellent chilled water cooling capacity, it also required a large lead time for chill-down. This chill-down generally took about 2 hours for a chilled water tank setpoint of 40 degrees Fahrenheit. The external and building environment, in which the experimental room was enclosed, influenced this. For example, as the outside air temperature and domestic water temperature fluctuated during the summer and winter, this chill-down time might vary by as much as 30 minutes either direction. During this chill-down time the fan and circulating pump were allowed to run. This cooled the room down below the steady state temperature. After the chiller cycled off at its setpoint the panel control algorithm was allowed to come on and calculate the three pattern control response factors for the current room conditions. After these parameters were calculated the fan system

was turned off and the panels and pattern control algorithm ran their course bringing the panel temperature up to the specified setpoint. During the time that the panels were attaining setpoint, the chiller was still allowed to cycle and the coil pump was on continuously. Only the **fan system was turned off** during this time. When the panel setpoints were reached, the fan system was again turned on and the system was allowed to reach a steady-state condition. Once a steady-state condition was judged to be reached, the energy balance phase of the experiment was begun. Steady-state conditions were determined by a manual observation of the room inlet and outlet temperatures. Generally speaking this time was about one hour from the second start of the fan system. Total experimental time from chill-down time to steady state conditions was on the order of 3 to 3.5 hours. For consecutive experiments this time was approximately 1 to 1.5 hours. As can be seen a large amount of the time was spent chilling the water.

Another sequence which reduced experimental time but "fooled" the control algorithm was as follows. The chiller and panels were energized at the same time to reach specified setpoints simultaneously. The problem here is that the pattern control response factors are calculated for normal room temperature inputs. This underestimates the pattern-control parameters required under actual experimental conditions.

Another experimental procedure, attempted but abandoned, indicated that for the current panel control algorithm, the heated panels were underpowered.

Panel control is discussed further in section 3.2. The chiller was allowed to reach steady state and with the **fan system on** (in contrast to the first procedure above), the panel control algorithm was started and the panels were allowed to reach setpoint. This increased experimental time threefold as the under-powered panels struggled to reach setpoints even at low air flow rates. The first sequence as described above was deemed most effective and used for the majority of the experiments.

Following is an experimental log with related observations for three experiments performed on 5/06/95. The observations point to some of the shortcomings of the facility and these will be addressed in Chapter 4.

Table 2.2 Experimental Sequence: Instantaneous Status Log

Experiment #1: 1.6" & 3" nozzles Uncapped					
	air measurement system		chilled water system		experimental room
time	fan(Δp)	nozzles	chiller	coil pump	panels/ri/ro
12:20	0.0	————	on(65°F)	off(0 gpm)	105/70/70 °F
2:30	0.0	70.4°F	off(40°F)	on(4 gpm)	105/83.5/79.8 °F
2:32	1.09	————	off(41°F)	on(4 gpm)	105/—/— °F
2:45	1.09	53.9°F	on(42°F)	on(4 gpm)	105/63.5/75.1 °F
3:17	1.09	50.2°F	off(39°F)	on(4 gpm)	105/58.7/72.2 °F
3:40	1.09	51.4°F	on(42°F)	on(4 gpm)	105/58.0/71.7 °F
3:42	0.0	51.0°F	on(42°F)	on(4 gpm)	105/58.2/71.6 °F

Experiment #1: Observations

- Air leakage problems at the air-handler and access doors to the measurement box.
- Panel setpoint is 105 °F, Actual temperatures are between 104.20-104.97 °F.
- Thermal gradient in vertical according to thermocouple readings.
- Fan vibration is being transferred on to the experimental room.

Experiment #2: 7" nozzle Uncapped					
	air measurement system		chilled water system		experimental room
time	fan(Δp)	nozzles	chiller	coil pump	panels/ri/ro
3:46	0.0	57.2 °F	on(41 °F)	on(0 gpm)	105/78.0/72.9 °F
3:49	0.51	52.3 °F	on(41 °F)	on(4 gpm)	105/57.7/72.4 °F
4:26	0.51	49.7 °F	off(39 °F)	on(4 gpm)	105/53.2/61.6 °F
4:49	0.51	51.1 °F	on(42 °F)	on(4 gpm)	105/53.9/61.7 °F
4:52	0.0	50.2 °F	on(42 °F)	on(4 gpm)	105/53.8/61.6 °F

Experiment #2: Observations

- Air leakage less of a problem. Barely noticeable at measurement box.
- Less fan heat transferred to air. Better fan operating point.
- Panel setpoint is 105 °F, actual temperatures are 99.6-104.5 °F.
- Panel at inlet cannot maintain setpoint at the higher flow rates. Control algorithm needs to allow for this. This panel is washed with the chilled air.
- Room vibration is barely detectable.
- Laboratory temperature is 70 °F
- Panel at room inlet is still dropping, currently 91.35 °F. All other panels have stabilized between 99.6-104.4 °F. Panels are under-powered.

Experiment #3: 3" nozzle Uncapped					
	air measurement system		chilled water system		experimental room
time	fan(Δp)	nozzles	chiller	coil pump	panels/ri/ro
5:50	0.0	61.9°F	off(41 °F)	on(4 gpm)	105/81.4/78.6 °F
5:53	1.12	(——)	off(41 °F)	on(4 gpm)	105/57.7/72.4 °F
6:59	1.12	51.6 °F	on(42 °F)	on(4 gpm)	105/57.7/72.7 °F
7:00	0.0	51.2 °F	on(42 °F)	on(4 gpm)	105/57.7/72.7 °F

2.7.1 Experimental Startup and Shutdown

The following list summarizes startup and shutdown procedures required for each experimental session.

Startup

1. Open water main gate valve.
2. Switch air-handler, water source heat pump, panel and circulating pump breakers to ON position.
3. Check circulating pumps for proper operation proper connections.
4. Check storage tank water level.
5. Open heat pump water source regulating ball valve to 50% position.
6. Flip all chiller control switches to auto position including main chiller switch to start heat pump.
7. Check measurement box nozzle arrangement and ensure all access doors are secured.
8. Check inclined manometer fluid level.
9. Turn air-handler switch to ON position.
10. Turn Fluke Datalogger ON.
11. Turn IBM PC ON and start MSDOS QBASIC.
12. Run Control.bas program to start panel warmup routines.
13. Check sump pump for proper operation while chiller is operating.

Shutdown

1. Turn chiller and air-handler OFF.
2. Turn fan-coil circulating pump OFF.
3. Type [control] [break] at IBM PC terminal.
4. Copy experiment data file to floppy disk and turn IBM PC OFF.
5. Turn panel, heat pump, air-handler and circulating pump breakers OFF.
6. Close main water gate valve OFF before leaving facility

2.8 Experimental Uncertainties

Final experimental results and conclusions should be viewed from the perspective of a reasonable error analysis. The variation of the measured value from its true value is the experimental error. There are primarily two types of experimental errors, systematic and random. Systematic errors affect the accuracy of the measured value but each experimental sample is affected in the same way. Instrument drift in one direction from the actual value is an example. On the other hand variations in the measured value on either side of the true value are the result of random errors. These errors result from the inability to control all variables affecting the measurement of a specific value. A normal distribution is assumed for these random errors .

For the study at hand, three forms of experimental uncertainty are investigated. Individual measurements of quantities such as temperature, power, and volumetric flow rate involve experimental error. Spatial averages of these quantities, such as average inlet temperature, compound the individual measurement errors. Finally, these errors are further compounded for calculated quantities, such as room air heat gain. The uncertainty associated with the calculation of air heat gain will be discussed in chapter 3, section 3.3.1.

2.8.1 Volumetric Flow Rate Uncertainty

Volumetric flow rate was measured in accordance with ASHRAE Standard 51-1985, Laboratory Methods of Testing Fan for Rating. This Standard outlines, in detail, the errors introduced by direct measurement of volumetric flow rate

according to the prescribed method. Variables affecting this measurement include the following: nozzle discharge coefficient, fan speed, area at measuring station, differential pressure and fan pressure. The uncertainty for determining volumetric flow rate in equation form is as follows:

$$e_Q = [e_c^2 + e_A^2 + (e_f/2)^2 + (e_p/2)^2 + e_N^2]^{1/2} \quad [2.1]$$

where,

$$e_c = \text{nozzle discharge coefficient error} = 0.012$$

$$e_A = \text{area error} = 0.005$$

$$e_f = \text{differential pressure error} = 0.05$$

$$e_p = \text{fan static pressure error} = 0.05$$

$$e_N = \text{fan speed} = 0.005$$

thus,

$$\begin{aligned} e_Q &= [0.012^2 + 0.005^2 + (0.05/2)^2 + (0.05/2)^2 + 0.005^2]^{1/2} \quad [2.1a] \\ &= 0.038 = \pm 3.8\% \end{aligned}$$

2.8.2 Temperature Measurement Uncertainty

The temperature measurements (i.e., nozzle, room inlet, room outlet, and panels), are susceptible to error via the Type T thermocouple wire properties (± 0.9 °F), cold junction compensation (± 0.1 °F), and the emf voltage (± 0.9 °F). Adding the errors in quadrature, due to the random nature of these errors:

$$e_T = [0.9^2 + 0.1^2 + 0.9^2]^{1/2} = \pm 1.3 \text{ °F} \quad [2.2]$$

2.8.3 Panel Power Uncertainty

Panel power is a function of line voltage and panel resistance. Fluctuations in line voltage during the course of an experiment ranged from two to three volts. These voltage fluctuations introduced uncertainties on the order of $\pm 2.5\%$ for an average voltage reading of 121.6 volts. The voltmeter was a negligible source of error on the order of $\pm 0.08\%$. Ohmmeter precision limits were $\pm 0.1\Omega$. This reflects an uncertainty of $\pm 0.125\%$ for an average panel resistance of 79.5Ω . The uncertainty introduced by the increased Ni-Cr wire temperature was assumed to be negligible. The overall panel uncertainty can thus be calculated as follows:

$$e_{\text{panel}} = [(2 \cdot e_{\text{volt}})^2 + (e_{\text{res}})^2]^{1/2} \quad [2.3]$$

where,

$$e_{\text{volt}} = \text{voltage fluctuation uncertainty} = 2.5\%$$

$$e_{\text{res}} = \text{ohmmeter precision} = 0.125\%$$

thus,

$$e_{\text{panel}} = \pm 5.15\% \quad [2.3a]$$

2.8.4 Spatial Average Uncertainty

One other potential source of error is spatial uncertainty due to limited local measurements used in determining average values. Room inlet and outlet temperatures were measured via the thermocouple arrangement shown in Figure

2.10. There was a vertical variation as is demonstrated in Figure 2.11. For the 1, 5 and 25 ach experiments, average inlet temperatures were 72.5, 57.3 °F and 52.3 °F, respectively. Figure 2.11 shows the vertical temperature gradient for these three flow rates.

The calculation of spatial uncertainty is more estimation than explicit analytical theory. For the current study, an estimate of inlet temperature spatial uncertainty will be the average inlet temperature plus or minus the range of measured inlet temperatures. Thus the spatial uncertainty for the room inlet temperature is reported as follows:

1 ach experiment: $72.5 \pm 7.7^\circ\text{F}$
5 ach experiment: $57.3 \pm 0.36^\circ\text{F}$
25 ach experiment $52.3 \pm 0.19^\circ\text{F}$

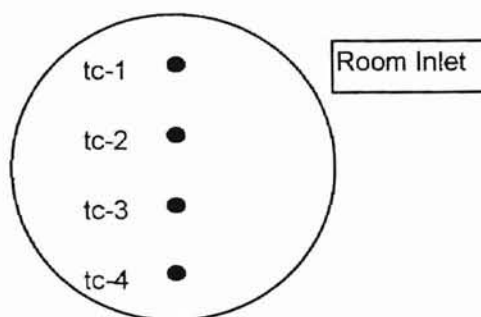


Figure 2.10 Room Inlet Temperature Thermocouple Arrangement

The large deviation that occurs for the 1 ach experiment serves warning that this data is not accurate enough to be useful. These deviations at low flow rates are discussed further in chapter 3, section 3.3.3.2. The spatial average

uncertainty is combined with the individual measurement uncertainty by adding in quadrature as follows:

$$e_{T,1ach} = [(1.3)^2 + (7.7)^2]^{1/2} = \pm 7.8 \text{ } ^\circ\text{F} \quad [2.4a]$$

$$e_{T,5ach} = [(1.3)^2 + (0.36)^2]^{1/2} = \pm 1.35 \text{ } ^\circ\text{F} \quad [2.4b]$$

$$e_{T,25ach} = [(1.3)^2 + (0.19)^2]^{1/2} = \pm 1.31 \text{ } ^\circ\text{F} \quad [2.4c]$$

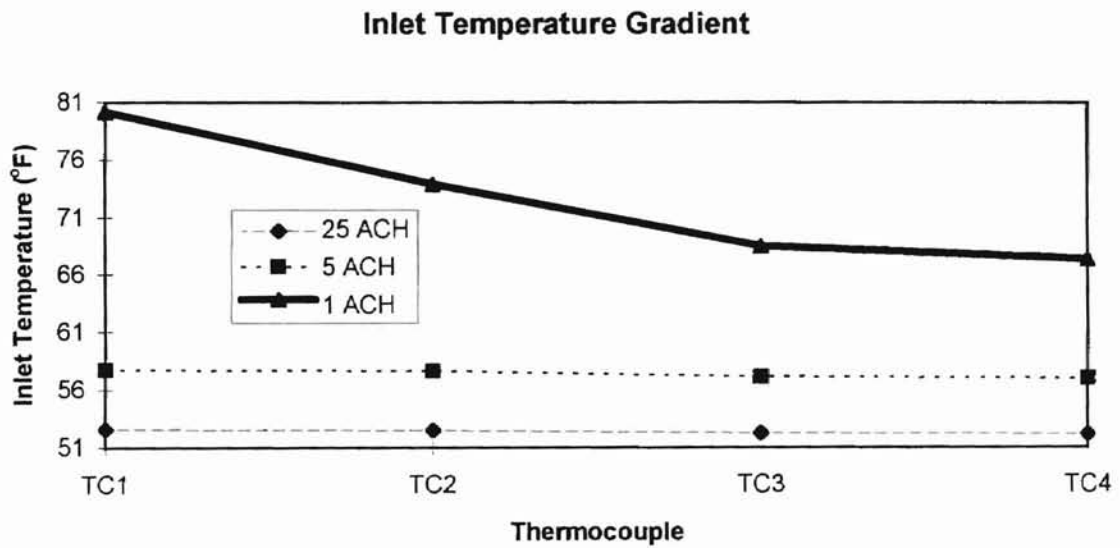


Figure 2.11 Room Inlet Temperature Gradient

CHAPTER THREE - RESULTS AND ANALYSIS

3.1 Summary of Experiments

Results are presented here for the initial experiments performed in the convective heat transfer experimental facility. Experimental averages and transient versus steady-state conditions are discussed with an emphasis being placed on facility heat balance performance.

Seventeen experiments are summarized in Table 3.1. **A subset of these experiments will receive particular attention (i.e., the 5,10, 15, 20 & 25 ach experiments).** The experiments shown in Table 3.1 cover room airflows between 28 and 820 cfm. For each experiment the following average values are reported: inlet and outlet velocity, air density, mass flow rate, volumetric flow rate, air changes per hour, inlet and outlet temperature, nozzle temperature, passive wall, ceiling and floor temperatures and panel temperature. Results from all seventeen experiments are given in Tables 3.2 and 3.3. Additionally, for the subset of experiments mentioned above, transient behavior versus steady-state behavior was investigated. Also, a number of representative fluid flow parameters are investigated and reported in Table C.2. Finally, an investigation of experimental errors is provided with their related impact on overall experimental facility performance.

Table 3.1 Overview of Experiments.

	File Name	Panel Temp.	Delta P	Flow Rate	ACH	Panel Power	Nozzle Set-up
1	E012895A	105 ^o F	.20	562	17.5	5369	7",3"&1.6"
2	E022595B	105 ^o F	.52	788	24.6	5369	7" & 1.6"
3	E030495	105 ^o F	.49	727	22.7	5559	7"
4	E050695A	105 ^o F	1.09	257	8	4772	1.6"&3"
5	E050695B	105 ^o F	.51	739	23.1	5724	7"
6	E050695C	105 ^o F	1.12	200	6.25	4239	3"
7	E080595A	100 ^o F	.40	806	25.2	5508	7",3"&1.6"
8	E080595B	100 ^o F	1.12	200	6.25	3985	3"
9	E081295A	98 ^o F	.52	746	24	5204	7"
10	E081295B	95 ^o F	1.20	28.3	.88	2335	1.6"
11	E082695	95 ^o F	.45	818	25.6	5255	7" & 3"
12	E090995	100 ^o F	.45	819	25.6	5610	7" & 3"
13	E091695	100 ^o F	.40	652	20.4	5470	7"
14	E091795A	100 ^o F	.10	324	10.1	4582	7"
15	E091795B	100 ^o F	.225	488	15.2	5166	7"
16	E091795C	100 ^o F	.75	163	5.1	3770	3"
17	E110495	100 ^o F	.75	164	5.1	3440	3"

Refer to the following in reference to Table 3.1:

- Panel Temp. - Panel setpoint (^oF)
- Delta P - Pressure differential across nozzle bank (inches of H₂O)
- Flow Rate - Measured volumetric flow rate (ft³/min)
- ACH - Air changes per hour
- Panel Power- Power input to the heated panels (btu/hr)
- Nozzle Set-up - Indicates which nozzles were left uncovered for experiment

3.1.1 Data Analysis

A data analysis program was written to manipulate the large amounts of temperature data, calculate the volumetric flow rate based on the ASHRAE Standard 51-1985 equations and calculate the overall room heat balance. The program is listed in Appendix A. This BASIC computer program sorts each

experimental data file and assigns the temperature measurements to arrays for processing. Overall temperature spatial averages for passive surfaces, nozzle, and room inlet and outlet are calculated. These averages are then passed on to an Excel spreadsheet and representative air-flow and heat transfer numbers are calculated. The computer program also calculates the room volumetric flow rate, panel energy input and room air heat gain. Results for the seventeen experiments are summarized below. In addition to the measured temperatures, the data analysis program also requires the following inputs: panel setpoint, nozzle bank arrangement, pressure differential across the nozzle bank, fan static pressure, barometric pressure, the experimental code number, and sample values for the steady state averages. The sample values are pre-determined and correspond to fan on/fan off times for each experiment. The data analysis program is written in batch form to evaluate all seventeen experiments at once and write corresponding results to corresponding output files. This saved large amounts of time during results analysis. The program ran for about twenty minutes on a 66 mhz, 486DX2 personal computer, to parse and calculate data for all seventeen experiments.

3.1.2 *Experimental Averages*

Table 3.2 is a summary of the average temperature measurements for each experiment. The final 50 measurements were used as the averaging sample. This averaging period or "steady-state condition" will be investigated later. The average bulk air temperature was estimated as the average of the

room surface temperatures. This temperature is used to calculate the bulk air properties which are given in Table 3.3. Additionally, these average air properties are used in calculating the following dimensionless parameters for room airflow: Reynolds #, Prandtl #, Rayleigh #, Archimedes #, Grashof #, and Jet Momentum #. An overview of these characteristic parameters is reported in Appendix C.

Table 3.2 Average Temperatures (Degrees Fahrenheit).

EXP	T_{nzi}	T_{ro}	T_{ri}	T_{clg}	T_{fir}
1	53.53	65.94	57.56	73.74	73.31
2	55.82	66.37	59.46	71.12	73.92
3	54.90	64.15	57.51	68.74	71.70
4	51.39	71.47	58.00	80.33	76.45
5	50.98	61.57	53.83	67.08	69.90
6	51.47	72.73	57.70	81.58	77.10
7	51.18	60.46	53.98	65.14	67.81
8	51.04	70.66	57.81	78.64	74.32
9	51.33	60.85	54.32	65.73	68.08
10	53.96	77.19	72.37	80.60	77.81
11	49.16	57.65	52.05	61.42	63.55
12	49.26	58.49	52.20	63.05	65.60
13	49.05	60.85	52.88	67.93	68.45
14	48.00	67.18	55.38	77.45	73.87
15	48.28	62.33	52.83	72.60	70.56
16	50.26	72.03	57.75	80.41	75.58
17	52.27	74.22	62.11	80.46	76.99
EXP	T_{pni}	T_{swll}	T_{nwll}	T_{ewll}	T_{mavg}
1	103.68	72.53	71.17	72.45	72.64
2	103.59	71.77	69.87	71.07	71.55
3	102.93	69.58	67.69	69.01	69.35
4	104.59	78.00	78.35	79.67	78.56
5	101.70	67.61	65.46	67.03	67.42
6	104.87	79.18	79.77	80.81	79.69
7	97.84	65.85	63.68	65.05	65.50
8	99.90	76.79	76.26	77.87	76.78
9	96.56	66.32	64.10	65.52	65.95
10	95.06	79.59	79.51	80.37	79.57
11	93.08	62.28	60.36	61.42	61.81
12	97.05	63.92	61.49	62.98	63.41
13	98.53	67.45	64.65	66.67	67.03
14	99.71	74.53	73.07	75.03	74.79
15	99.02	69.73	67.53	69.37	69.96
16	99.80	77.76	77.62	79.52	78.18
17	99.78	78.71	78.67	80.25	79.02

Table 3.3 Average Air Properties.

EXP	RHO_i	RHO_o	RHO_{nzi}	RHO_{∞}	μ_i	μ_{∞}	α_i	α_{∞}	β_i	β_{∞}
1	0.0765	0.0751	0.0772	0.0740	1.204E-4	1.231E-4	0.8167	0.8450	0.00190	0.00185
2	0.0762	0.0750	0.0768	0.0741	1.207E-4	1.229E-4	0.8202	0.8429	0.00189	0.00185
3	0.0765	0.0754	0.0770	0.0745	1.204E-4	1.225E-4	0.8166	0.8387	0.00190	0.00186
4	0.0765	0.0742	0.0776	0.0730	1.204E-4	1.241E-4	0.8175	0.8567	0.00190	0.00183
5	0.0772	0.0758	0.0776	0.0748	1.197E-4	1.221E-4	0.8100	0.8350	0.00191	0.00186
6	0.0765	0.0739	0.0776	0.0728	1.204E-4	1.243E-4	0.8170	0.8589	0.00190	0.00182
7	0.0771	0.0760	0.0776	0.0752	1.197E-4	1.218E-4	0.8103	0.8314	0.00191	0.00187
8	0.0765	0.0743	0.0776	0.0733	1.204E-4	1.238E-4	0.8172	0.8531	0.00190	0.00183
9	0.0771	0.0760	0.0776	0.0751	1.198E-4	1.219E-4	0.8109	0.8322	0.00191	0.00187
10	0.0740	0.0732	0.0771	0.0728	1.230E-4	1.243E-4	0.8445	0.8587	0.00185	0.00182
11	0.0775	0.0765	0.0780	0.0758	1.194E-4	1.211E-4	0.8069	0.8245	0.00192	0.00188
12	0.0774	0.0764	0.0779	0.0755	1.194E-4	1.214E-4	0.8071	0.8275	0.00192	0.00188
13	0.0773	0.0760	0.0780	0.0749	1.195E-4	1.221E-4	0.8083	0.8343	0.00192	0.00187
14	0.0769	0.0749	0.0782	0.0736	1.200E-4	1.235E-4	0.8128	0.8492	0.00191	0.00184
15	0.0773	0.0757	0.0781	0.0744	1.195E-4	1.226E-4	0.8082	0.8399	0.00192	0.00186
16	0.0765	0.0741	0.0778	0.0730	1.204E-4	1.241E-4	0.8171	0.8559	0.00190	0.00183
17	0.0758	0.0737	0.0774	0.0729	1.212E-4	1.242E-4	0.8251	0.8576	0.00188	0.00182

Please note that the subscripts i , o , nzi , and ∞ refer to air properties calculated at the room inlet, room outlet, flow nozzle entrance and room air average temperatures. Units for the above properties are reported in the Nomenclature section of the thesis.

3.2 Transient Versus Steady State

Facility heat balance calculations require that the following question be evaluated: Did the facility reach a sufficiently steady state condition? Figure 3.1 shows a room interior elevation and the heated panel arrangement. Figure 3.2 shows panel temperature versus time for the 25 ach (820 cfm) & 5 ach (165 cfm) experiments. By inspection of Figure 3.2, a number of panels are unable to

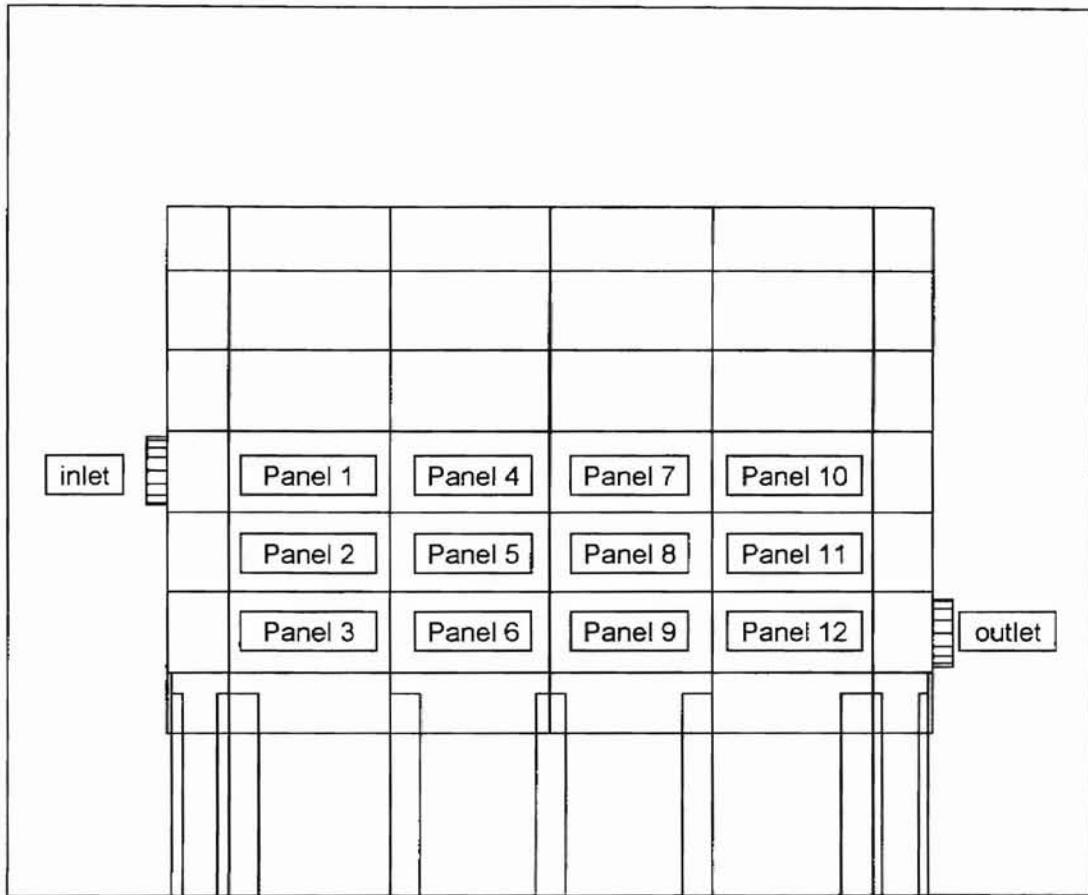


Figure 3.1 Experimental Room Interior Elevation, Heated Panel Layout

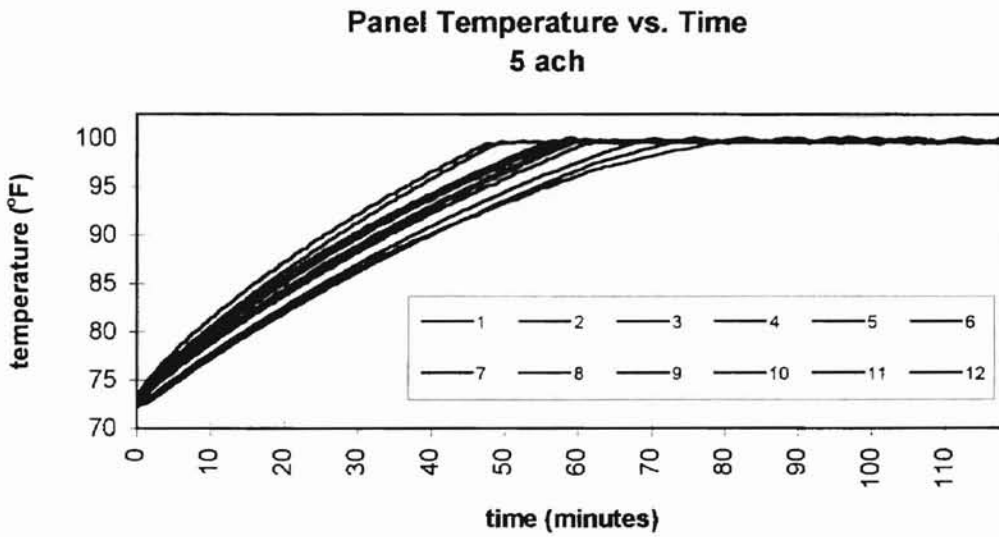
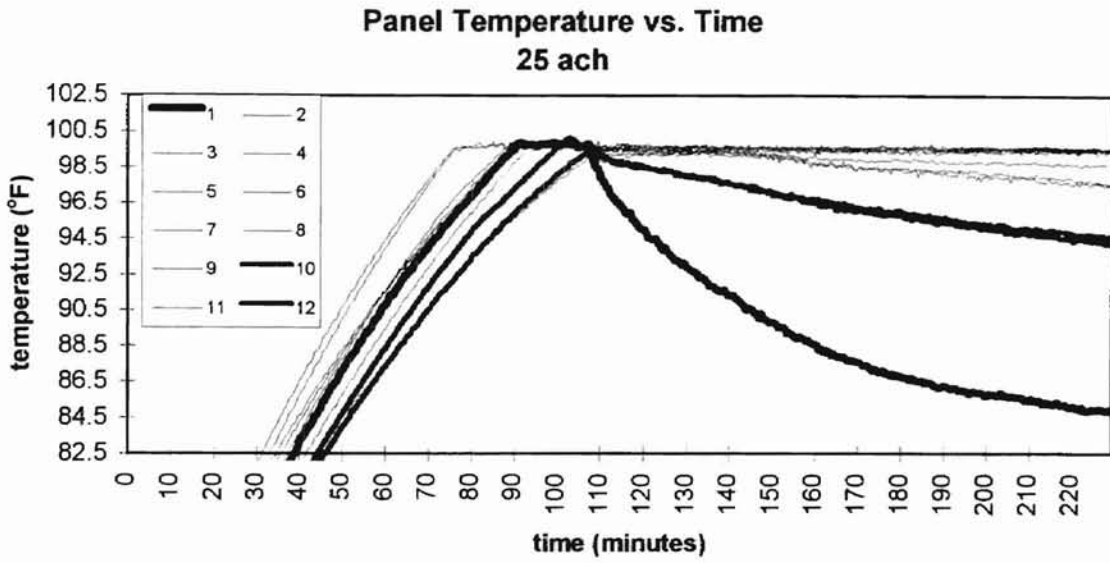


Figure 3.2 Panel Temperature vs. Time - 100°F Setpoint, 820 cfm & 165 cfm.

maintain the setpoint at higher volumetric flow rates, whereas, at the lower volumetric flow rates the setpoint is maintained (i.e., refer to figures 3.1 and 3.2).

To investigate this condition, panel power duty cycles were calculated for the last 20 minutes of the 5 and 25 ach experiments. This time corresponds to the last 250 samples at 5 seconds per sample. Table 3.4 gives these results.

Table 3.4 Heated Panel Power Duty Cycles

panel	1	2	3	4	5	6	7	8	9	10	11	12
25 ach	.75	.75	.75	.74	.74	.74	.75	.71	.74	.75	.69	.75
5 ach	.46	.60	.56	.38	.48	.56	.42	.42	.45	.43	.36	.50

It is evident, at the higher flow rates, that certain panels are unable to maintain their desired setpoints. The panels with depressed temperatures are essentially washed by the inlet jet at the higher flow rates or are located adjacent to an area of cool air recirculation and build-up (i.e., panel 12 located adjacent to where the inlet jet impinges on the far wall).

Two inferences can be made regarding the panels and their performance from an examination of Figure 3.2 and Table 3.4. First, the panel control strategy is problematic as only a 75% duty cycle is realized even at the high volumetric flow rate. Second, the panels are sufficiently powered to control around the desired setpoint at the lower flow rates. The panel control algorithm should be revised to allow for a higher duty cycle.

Figures 3.3 - 3.8 show nozzle, inlet, and outlet temperatures as functions of time. By inspection, the nozzle temperature indicates a sensitivity to chiller cycling. The room inlet and outlet temperatures show a somewhat dampened effect of chiller cycling on temperature. This was true for all experiments.

The six experiments shown in Figures 3.3 -3.8 represent a subset of experiments, all performed at a panel setpoint of 100 °F at 5, 10, 15, 20, and 25 ach. The first graph in each figure shows temperature versus time from panel control program start to system shutdown. The marked discontinuity indicates fan start. Those experiments not indicating this discontinuity were the second or third experiments in a series. The second graph shows nozzle, inlet, and outlet temperatures during the averaging period (i.e., the last fifty samples). Additionally, linear curve fit equations are displayed for all three temperatures, as well as, the inlet to outlet temperature difference. These equations indicate that the experiments would have benefited from a longer run time. However, it should be noted that the temperature difference equations show a relatively flat line and very little change over time. This is important to note, in that it is this delta T that is used to calculate the air heat gain for the overall facility heat balance.

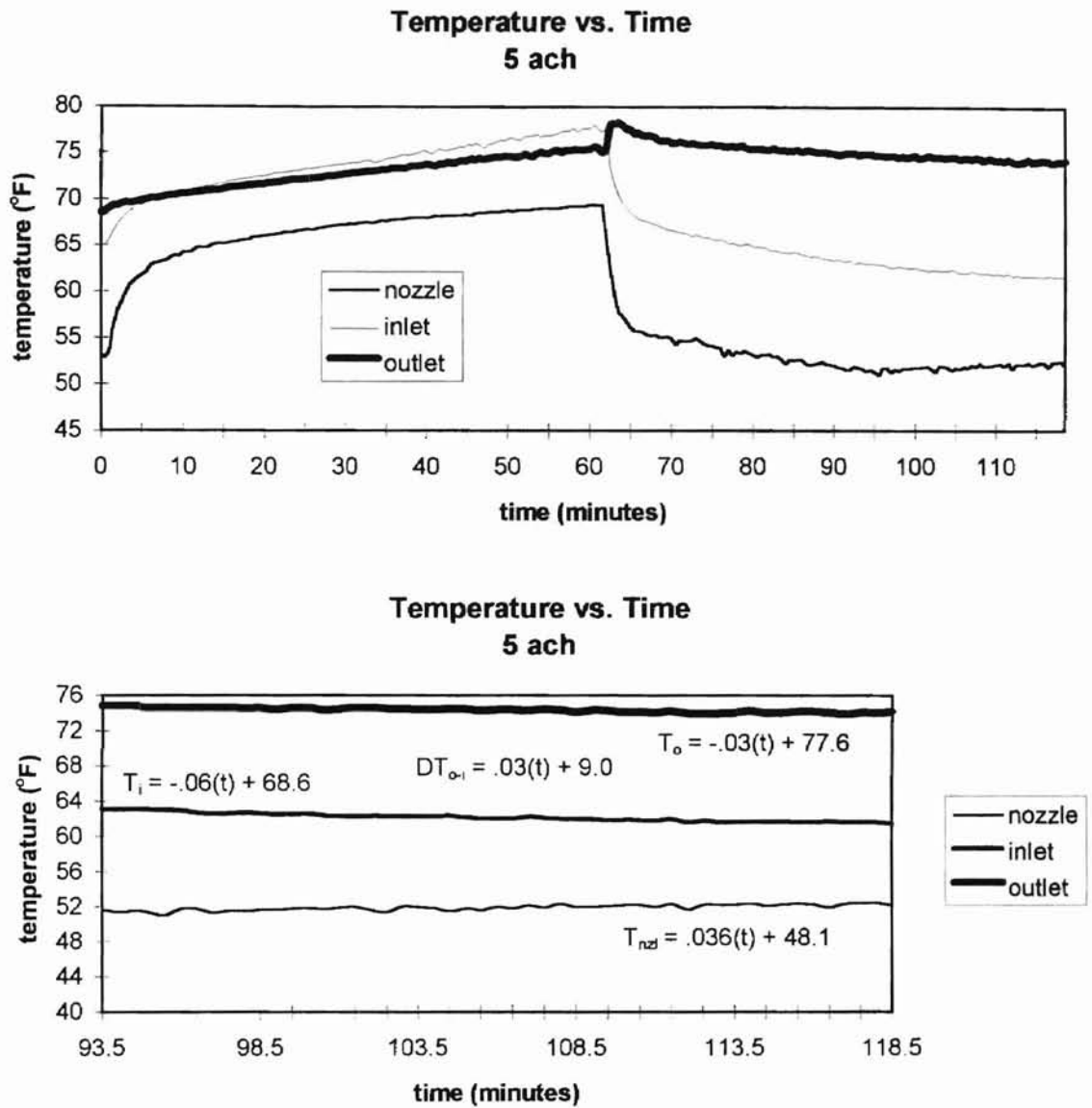


Figure 3.3 Nozzle, Room Inlet, and Outlet Temperatures vs. Time (5 ach w/foil)

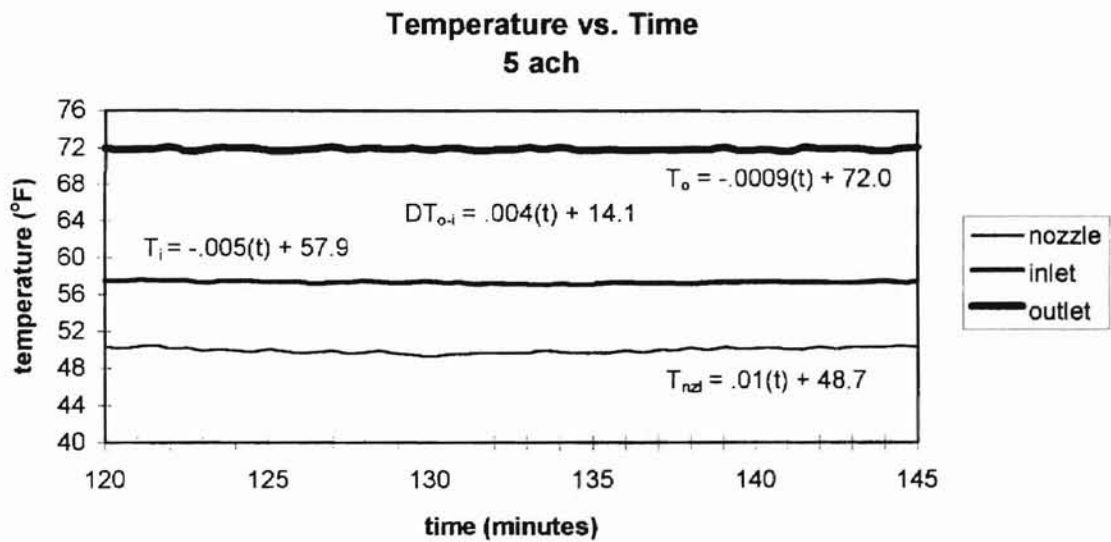
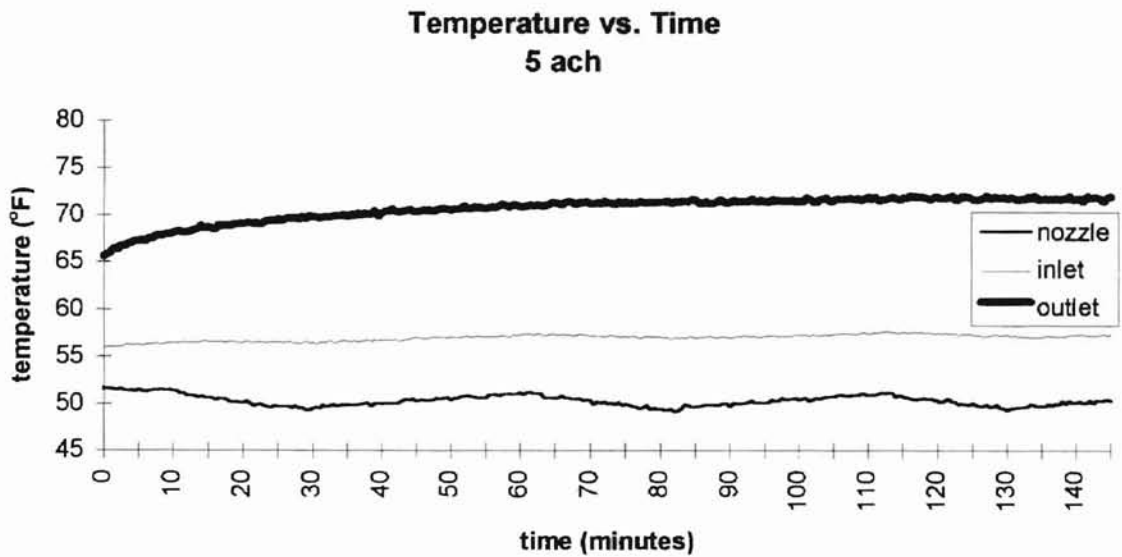


Figure 3.4 Nozzle, Room Inlet, and Outlet Temperatures vs. Time (5 ach)

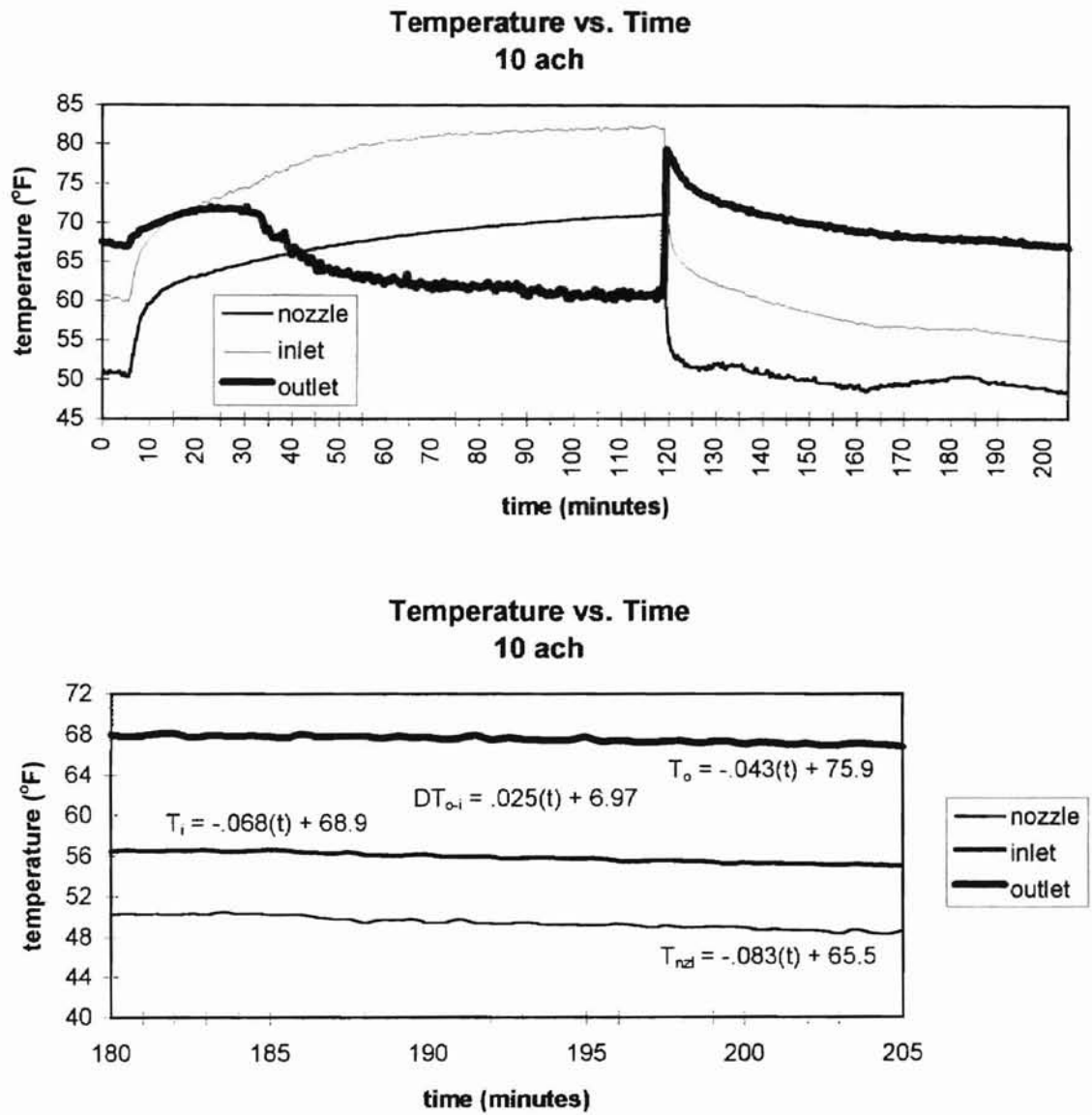


Figure 3.5 Nozzle, Room Inlet, and Outlet Temperatures vs. Time (10 ach)

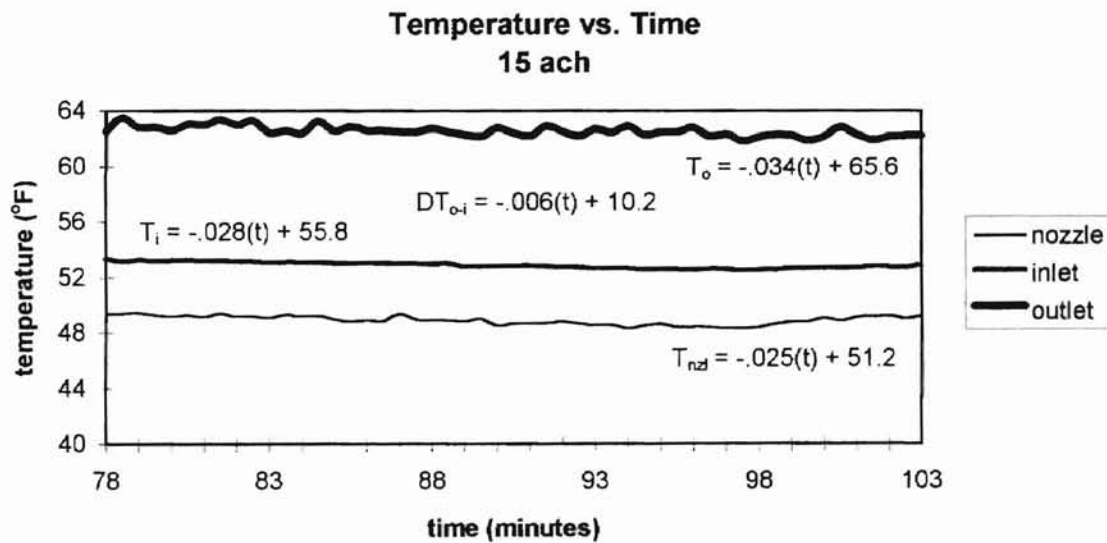
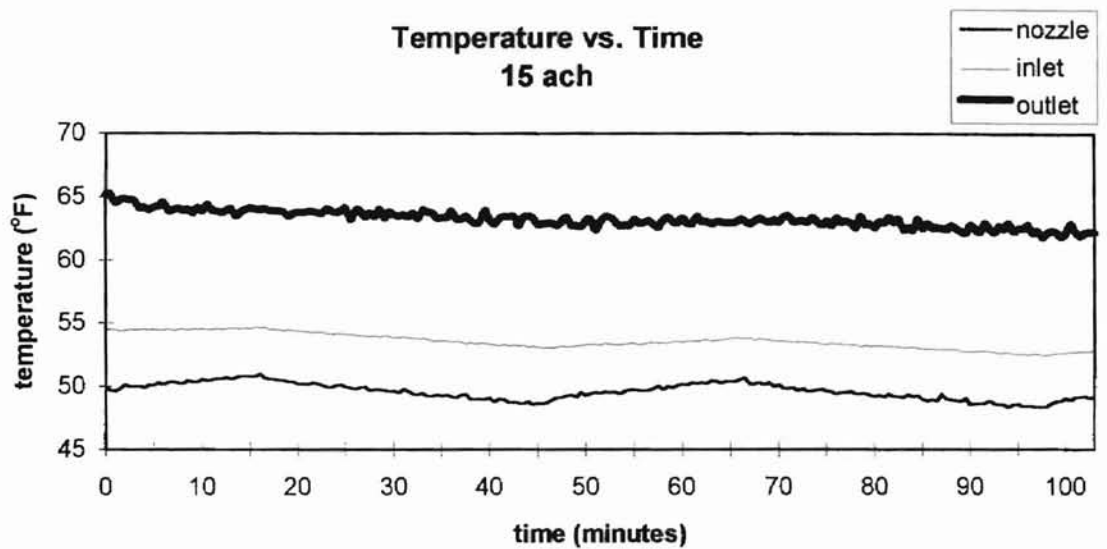


Figure 3.6 Nozzle, Room Inlet, and Outlet Temperatures vs. Time (15 ach)

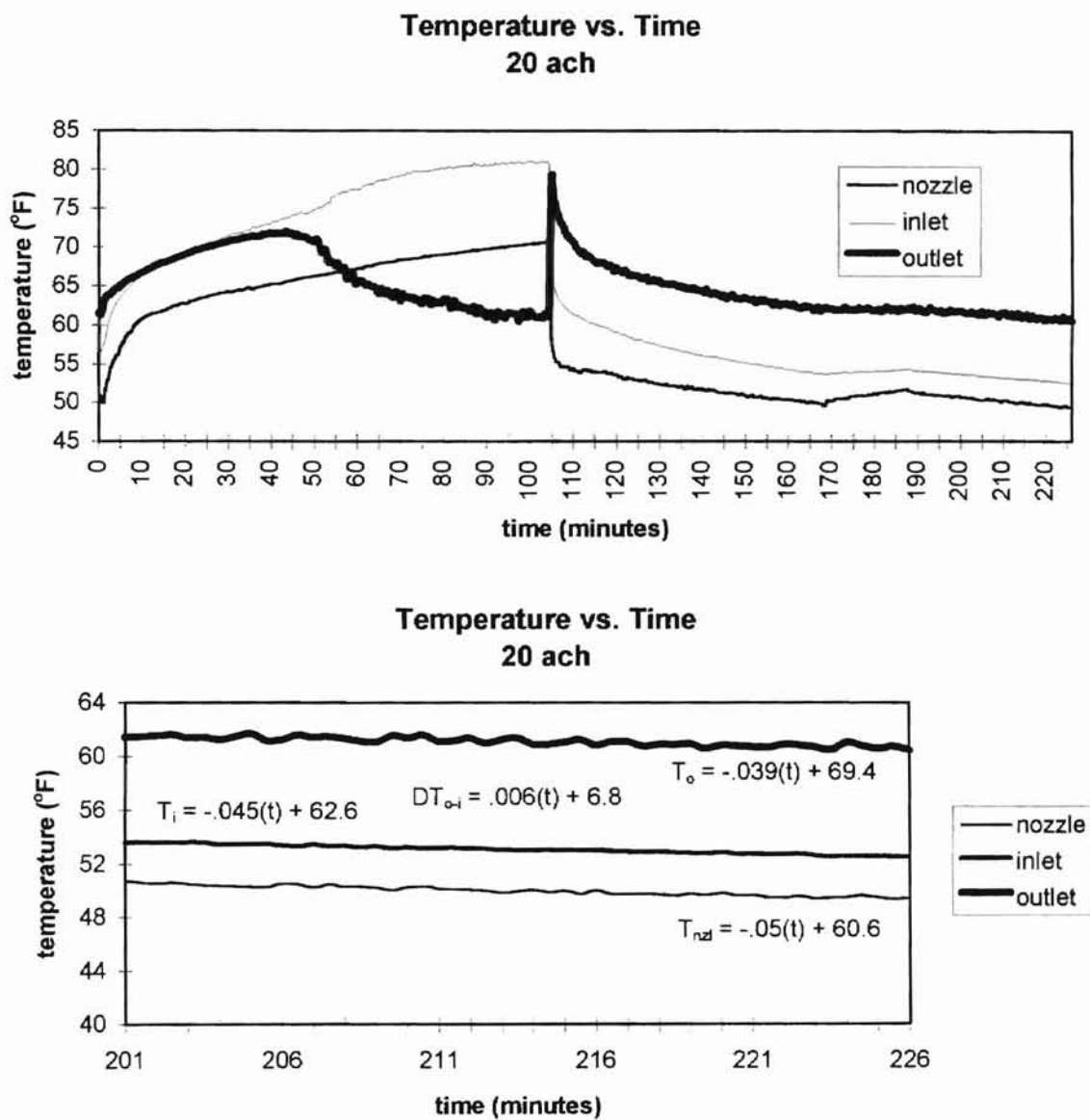


Figure 3.7 Nozzle, Room Inlet, and Outlet Temperatures vs. Time (20 ach)

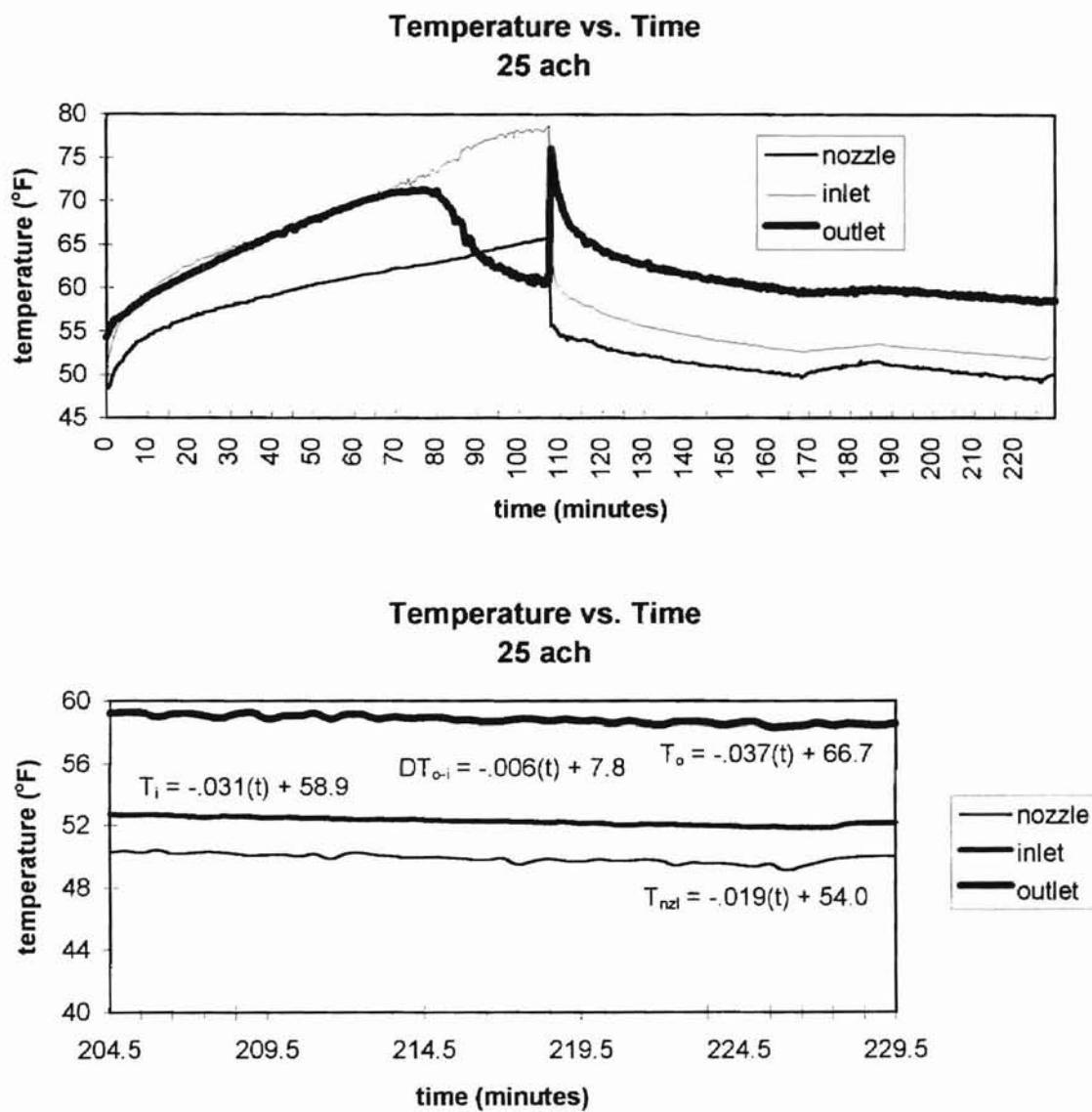


Figure 3.8 Nozzle, Room Inlet, and Outlet Temperatures vs. Time (25 ach)

3.3 Room Heat Balance

Satisfactory facility performance and future usefulness is dependent upon the facilities' ability to achieve an overall heat balance. This heat balance, for a given time period, is given in equation form as follows:

$$Q_{\text{air},i} = \Sigma Q_{\text{panel},i} - \Sigma Q_{\text{cond},i} \quad [3.1]$$

Where

$$Q_{\text{air}} = \text{air heat gain} = \dot{m} c_p (T_o - T_i) \quad [3.2]$$

$$Q_{\text{panel}} = \text{total panel power input} = \sum_{j=1}^{12} (V^2/R_j) \quad [3.3]$$

R_j equals electrical resistance of panel j .

$$Q_{\text{cond}} = \text{room conduction heat loss} = \sum_{j=1}^{12} A_j (T_{\text{si}} - T_{\text{so}}) / R_j \quad [3.4]$$

R_j equals thermal resistance of surface j .

The above equation can be simplified if it is assumed that back losses (Q_{cond}) are negligible (Sanders, 1995). Thus energy input to the panels should equal the air heat gain from room inlet to outlet.

3.3.1 Air Heat Gain Uncertainty

Air heat gain is calculated according to the following equation:

$$Q_{\text{air}} = \rho \dot{V} c_p \Delta T \quad [3.5]$$

where,

$$\Delta T = T_{\text{outlet}} - T_{\text{inlet}} \quad [3.6]$$

In equation form, the uncertainty due to this derived quantity is as follows:

$$e_{Q_{air}} = [e_{vfr}^2 + (e_{\Delta T}/\Delta T)^2]^{1/2} \quad [3.7]$$

where,

$$\begin{aligned} e_{vfr} &= \text{volumetric flow rate uncertainty from section 2.8.1} \\ &= 0.038 \end{aligned}$$

$$\begin{aligned} e_{\Delta T} &= \text{uncertainty due to } \Delta T \text{ between room inlet and outlet} \\ &= [e_{tin}^2 + e_{tout}^2]^{1/2} \end{aligned} \quad [3.8]$$

The uncertainty due to the inlet-to-outlet temperature difference is dependent upon the ΔT for each experiment.

Example calculations for the 1, 5 and 25 ach temperature difference uncertainties are offered as follows:

$$e_{\Delta T,1} = \pm [(7.8)^2 + (7.8)^2]^{1/2} = \pm 11.0^\circ\text{F} \quad [3.8a]$$

$$e_{\Delta T,5} = \pm [(1.35)^2 + (1.35)^2]^{1/2} = \pm 1.91^\circ\text{F} \quad [3.8b]$$

$$e_{\Delta T,25} = \pm [(1.31)^2 + (1.31)^2]^{1/2} = \pm 1.85^\circ\text{F} \quad [3.8c]$$

For simplification the above calculation assumes inlet and outlet uncertainties are equal. While the above temperature uncertainties include the spatial measurement uncertainty, spot measurements at the room outlet showed these to be much smaller than room inlet variations. The overall air heat gain uncertainties are summarized for all seventeen experiments in Table 3.5. The shaded entries in Table 3.5 represent the six core experiments.

Table 3.5 Air Heat Gain Uncertainty by Experiment.

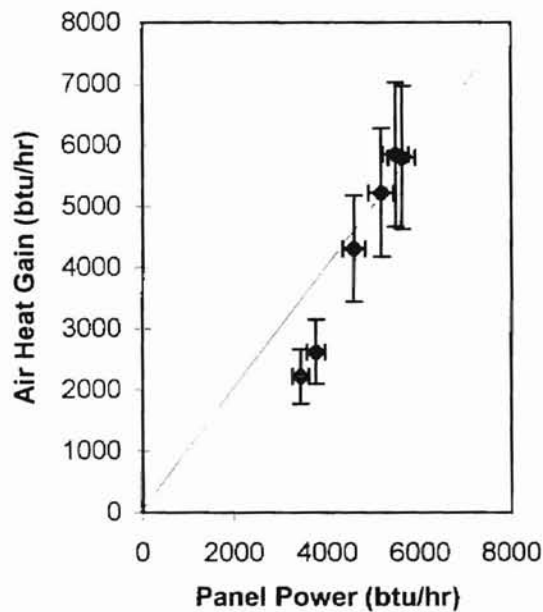
code	ach	T _{outlet} - T _{inlet} (°F)	air heat gain uncertainty
E012895A(1)	18	8.38	0.23
E022595B(2)	25	6.91	0.27
E030495(3)	23	6.65	0.28
E050695A(4)	8	13.47	0.15
E050695B(5)	23	7.74	0.24
E050695C(6)	6	15.02	0.13
E080595A(7)	25	6.47	0.29
E080595B(8)	6	12.85	0.15
E081295A(9)	24	6.53	0.29
E081295B(10)	1	4.82	2.28
E082695(11)	26	5.59	0.33
E090995(12)	25	6.29	0.30
E091695(13)	20	7.97	0.24
E091795A(14)	10	11.81	0.17
E091795B(15)	15	9.5	0.20
E091795C(16)	5	14.28	0.14
E110495(17)	5	12.11	0.16

3.3.2 Preliminary Heat Balance Results

Table 3.6 summarizes the panel power versus air heat gain values for all seventeen experiments. For the six core experiments (shaded entries in Table 3.6), air heat gain versus panel power is plotted in Figure 3.9. The line $y=x$ represents the ideal heat gain curve. The panel power uncertainties are represented by the horizontal error bars and the air heat gain uncertainties are represented by the vertical error bars. The lower flow rate experiments fall short of good agreement as the predicted uncertainties do not intersect the ideal curve.

Table 3.6 Summary of Panel Power and Air Heat Gain Values.

code	ach	panel power (btu/hr)	air heat gain (btu/hr)
E012895A(1)	18	5369	5328
E022595B(2)	25	5369	6045
E030495(3)	23	5559	5375
E050695A(4)	8	4772	3823
E050695B(5)	23	5724	6415
E050695C(6)	6	4239	3369
E080595A(7)	25	5508	5853
E080595B(8)	6	3985	2882
E081295A(9)	24	5204	5460
E081295B(10)	1	2335	1519
E082695(11)	26	5255	5155
E090995(12)	25	5610	5795
E091695(13)	20	5470	5852
E091795A(14)	10	4582	4313
E091795B(15)	15	5166	5224
E091795C(16)	5	3770	2621
E110495(17)	5	3440	2216

Air Heat Gain vs. Panel Power**Figure 3.9** Room Heat Balance - Air Heat Gain vs. Panel Power.

This condition is far from ideal and serves warning that not all experimental uncertainties have been calculated. Additionally, it may also emphasize that previous simplifying assumptions should be re-visited for overall heat balance impact. The following sections outline a number of problematic uncertainties that were difficult to quantify or would require substantial experimental verification.

3.3.3 Room Inlet Factors

3.3.3.1 Temperature and Velocity Gradient

As discussed in section 2.8, a vertical gradient at the room inlet was observed, especially at the lower volumetric flow rates. In fact, at these lower flow rates the top thermocouple followed the bulk air temperature. As shown in Figure 2.11 of section 2.8, at 5ach the inlet vertical temperature gradient was approximately 1°F. For a volumetric flow of 1 ach this vertical temperature gradient at the room inlet was approximately 12.5°F. The bulk air temperature of 79.57°F, for the 1 ach experiment, closely approximated the top room inlet thermocouple reading.

Additionally, velocity measurements were not taken across the room inlet. This is significant because most of the air movement occurs along the bottom of the 2' x 2' duct, even at volumetric flow rates as high as 15 ach (Spitler, 1991). This velocity gradient at the room inlet tends to compound the temperature gradient. Further experimentation is recommended to investigate the velocity gradient condition.

The effect the room inlet temperature gradient had on the temperature measurement has been estimated in section 2.8. While the air heat gain uncertainty reported in Table 3.5 accounts for these temperature gradients, as Figure 3.9 indicates, the heat balance results still do not agree within the predicted uncertainties at the lower flow rates.

3.3.3.2 Radiation Effects

Radiative communication to the room inlet thermocouple from surrounding surfaces is another source of possible air heat gain error. Welty (1969), Parker (1972), Siegel (1974) and ASHRAE HOF (1993) give the following fundamental relationships for thermal radiation in an enclosure with n diffuse-gray surfaces. This equation is derived from a development of the full matrix representation method for determining radiant exchange between surfaces and is developed fully in the above sources.

$$J_i = \varepsilon_i E_{b,i} + (1 - \varepsilon_i) \sum_{j=1}^n F_{ij} J_j \quad i = 1, 2, \dots, n \quad [3.9]$$

where

J = radiosity of surface j (Btu/hr-ft²)

ε_i = emittance of surface i

F_{ij} = view factor from surface i to surface j

$E_{b,i}$ = black body emissive power of surface i

The equation for black body emissive power is:

$$E_{b,i} = \sigma T_i^4 \quad [3.10]$$

where,

$$\sigma = \text{Stefan-Boltzman constant} = 0.1714 \times 10^{-8} \text{ btu/hr-ft}^2\text{-(}^\circ\text{R)}^4$$

finally,

$$q_{radi} = \frac{E_{bi} - J_i}{(1 - \epsilon_i) / \epsilon_i A_i} \quad [3.11]$$

where,

q_{radi} = Net radiation heat transfer from surface i

A_i = Area of surface i

The room is divided into 9 surfaces including the thermocouple (reference Appendix D). Table 3.7 tabulates the parameters used in equations 3.9, 3.10, 3.11. The following calculations are for the 5 ach (E091795C) experiment.

Table 3.7 Summary of Radiation Calculation Parameters

surface	$A_i(\text{ft}^2)$	ϵ_i	T_i ($^\circ\text{F}$)	explanatory notes
north wall	120.0	0.1	77.62	T_{north} measured w/ 6 tc's
south wall	117.82	0.1	77.76	T_{south} measured w/ 6 tc's
west wall	64.0	0.1	78.0	T_{west} estimated as T_i/i
east wall	160.0	0.1	79.52	T_{east} measured w/ 3 tc's
heated panels	96.0	0.9	100.0	T_{panel} equal to panel setpoint
inlet duct	2.18	0.9	57.75	T_{duct} estimated as T_{in}
floor	192.0	0.1	75.58	T_{floor} measured w/ 6 tc's
ceiling	192.0	0.1	80.41	T_{ceiling} measured w/ 6 tc's
thermocouple	8.52×10^{-5}	0.8	57.75	mounted at room inlet

substituting values from Table 3.7 into equation 3.10,

$$E_{tc} = 0.1714 \times 10^{-8} * 517.8^4 = 123 \text{ btu/hr-ft}^2 \quad [3.10a]$$

$$E_{north} = 0.1714 \times 10^{-8} * 537.6^4 = 143 \text{ btu/hr-ft}^2 \quad [3.10b]$$

$$E_{south} = 0.1714 \times 10^{-8} * 537.8^4 = 143 \text{ btu/hr-ft}^2 \quad [3.10c]$$

$$E_{west} = 0.1714 \times 10^{-8} * 538.0^4 = 144 \text{ btu/hr-ft}^2 \quad [3.10d]$$

$$E_{east} = 0.1714 \times 10^{-8} * 540.0^4 = 146 \text{ btu/hr-ft}^2 \quad [3.10e]$$

$$E_{panel} = 0.1714 \times 10^{-8} * 560.0^4 = 169.0 \text{ btu/hr-ft}^2 \quad [3.10f]$$

$$E_{duct} = 0.1714 \times 10^{-8} * 514.0^4 = 120.0 \text{ btu/hr-ft}^2 \quad [3.10g]$$

$$E_{floor} = 0.1714 \times 10^{-8} * 536.0^4 = 141 \text{ btu/hr-ft}^2 \quad [3.10h]$$

$$E_{ceiling} = 0.1714 \times 10^{-8} * 540.0^4 = 146 \text{ btu/hr-ft}^2 \quad [3.10i]$$

Substituting the emissivities, black body emissive powers and the view factors into equation 3.9 yields a system of n linear equations and n unknowns. Thus the radiosities used in equation 3.11 can be determined. Substituting the radiosities into equation 3.11 yields the net radiative heat transfer for the surface of interest. For this example calculation we wish to determine the net radiation heat transfer from the room inlet thermocouple. Using Microsoft Excel matrix solving functions and estimated view factors, the system of linear equations was solved for the radiosities. The estimated view factors are reported in Appendix E.

For the thermocouple net radiation heat transfer:

$$\begin{aligned} q_{rad,tc} &= (123 - 142.82)/[(1-0.9)*(0.9*8.52 \times 10^{-5})] & [3.11b] \\ &= -0.00252 \text{ btu/hr} \end{aligned}$$

By observation of equation 3.11b, the net radiation from the thermocouple to each surface is negative in sign. This negative sign indicates radiation heat

transfer *to* the thermocouple at the room inlet *from* the surrounding surfaces.

Dividing the net radiation heat transfer rate by the thermocouple surface area the radiative flux is:

$$q''_{\text{rad,tc}} \approx -0.00252/8.52 \times 10^{-5} = -12.0 \text{ btu/hr-ft}^2 \quad [3.12]$$

The rate of heat gain by radiation to the thermocouple is equated to the rate of heat loss by convection. In equation form:

$$q''_{\text{rad,tc}} = h_{\text{conv}}(T_{\text{air}} - T_{\text{tc}}) = 4.0 * (T_{\text{air}} - 57.75) \quad [3.13]$$

where,

$$h_{\text{conv}} \approx 4.0 \text{ btu/hr-ft}^2\text{-}^\circ\text{F (Welty et. al., 1969)}$$

$$T_{\text{tc,5ach}} = 57.75$$

thus,

$$T_{\text{air}} = 54.75 \text{ }^\circ\text{F} \quad [3.14]$$

Finally, for the above example, the resulting error in measured temperature is approximately 3.0°F. Referring to section 2.8 and modifying equations 2.2 and 2.4, the corrected inlet temperature uncertainty for the 5 ach experiment becomes:

$$e_{T,\text{corr}} = [(\pm 1.3^\circ\text{F})^2 + (\pm 3.0^\circ\text{F})^2 + (\pm 0.36)^2]^{1/2} = \pm 3.3^\circ\text{F} \quad [3.15]$$

Substituting this uncertainty into equation 3.8 and referring to equation 3.7, the air heat gain uncertainty for the 5 ach experiment is then modified as follows:

$$e_{Q_{\text{air,corr}}} = [(.038)^2 + (3.3/17.28)^2]^{1/2} = 0.195 \quad [3.16]$$

This calculation demonstrates the impact radiative communication had on the inlet temperature measurement and consequently the air heat gain uncertainty. This is summarized further in section 3.3.5.

Additionally, an upper limit check on the air temperature error is calculated by assuming the thermocouple is surrounded by the panel temperature. An expression for the radiant exchange between two gray surfaces that “see” only each other is given in equation 3.17. Substituting values from table 3.7 and equations 3.10a,f:

$$q_{rad,tc} = \frac{E_{tc} - E_{panel}}{\frac{1 - \epsilon_{tc}}{A_{tc}\epsilon_{tc}} + \frac{1}{A_{tc}F_{tc-panel}} + \frac{1 - \epsilon_{panel}}{A_{panel}\epsilon_{panel}}} \quad [3.17]$$

where,

$$\begin{aligned} F_{tc-panel} &= 1.0 \\ A_{panel} &= A_{room} = 944.0 \text{ ft}^2 \\ A_{tc} &= 8.52 \times 10^{-5} \text{ ft}^2 \end{aligned}$$

thus,

$$q_{rad,tc} = -0.0031 \text{ btu/hr} \quad [3.17a]$$

Dividing this value by the surface area of the thermocouple to obtain the radiative flux,

$$q''_{rad,tc} = -36.4 \text{ btu/hr-ft}^2 \quad [3.17b]$$

Substituting this value into equation 3.13 and solving for T_{air} , an upper limit of 9.2 °F is calculated. Thus the estimated inlet temperature error of 3.0 °F due to radiation effects is reasonable as it falls below the upper bound.

3.3.4 Air Heat Gain Modification

3.3.4.1 Room Transient Effects

As per the discussion in section 3.2, the experiments could have benefited from a longer run time. While it has not been verified, the experimental data seems to indicate that a relatively long run time would be required to bring the room inlet temperature in line and thus improving the overall room heat balance. Time constraints did not allow a full investigation of this. However, with the spot measurements indicating room stratification, the question of a non-steady state conditions at these lower flow rates was investigated. Thus ceiling temperatures were plotted for the 5 ach experiment. Figure 3.10 shows ceiling temperature versus the last ten minutes of the experiment (i.e., the averaging period of 50 samples).

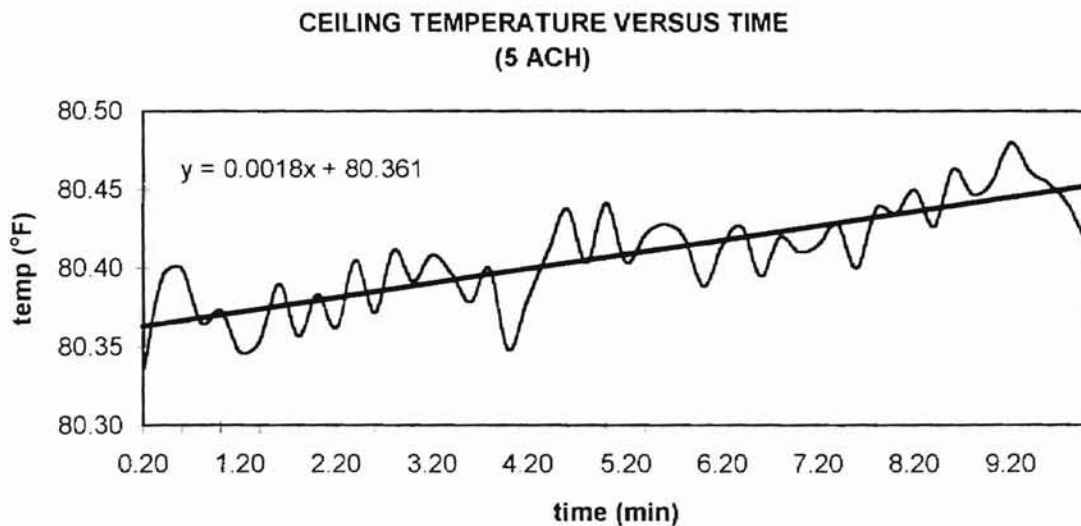


Figure 3.10 Ceiling Temperature vs. Time.

The positive slope of the line in Figure 3.10 demonstrates that the room had not reached a true steady-state condition. This confirms what was reported in Section 3.1. The increasing ceiling temperature and the spot measurements indicate a stratified condition. For this non-steady state condition the buoyancy driven flow is supplied and returned below the stratification line within the room. The heat from the panels rises into this stratified region and the buoyancy driven flow immediately drops upon entering the room from the side wall inlet and leaves at the lower side wall outlet without ever mixing with the upper stratified air. At true steady-state this room stratification should not exist.

The following equation estimates the amount of heat being transferred to the stratified region for the 5 ach experiment. The following accounts for the mass of the air in upper half of the room and the mass of room construction components (i.e., two-by-twelve framing).

$$q_{\text{tran,5ach}} = m_{\text{air}}c_{p,\text{air}}(dT/dt) + m_{\text{room}}c_{p,\text{framing}}(dT/dt) \quad [3.18]$$

where,

q_{tran} = transient heat transfer to stratified region for 5 ach experiment

m_{air} = mass of air in stratified region = $\rho_{\text{air}}V_{\text{strat}} = 0.075 \text{ (lbm/ft}^3\text{)} * 960 \text{ (ft}^3\text{)}$

m_{room} = mass of room components in stratified region

$$= 25 \text{ (ft}^3\text{)} * 32.0 \text{ (lbm/ft}^3\text{)} = 800 \text{ lbm}$$

$c_{p,\text{air}} = 0.24 \text{ (btu/lbm-}^\circ\text{F)}$

$c_{p,\text{framing}} = 0.33 \text{ (btu/lbm-}^\circ\text{F)}$

dT/dt = slope of curve shown in Figure 3.10 = $0.0018 \text{ (}^\circ\text{F/min)}$

thus,

$$q_{\text{tran},5\text{ach}} \approx 2.0 \text{ btu/hr} + 28.5 \text{ btu/hr} = 30 \text{ btu/hr} \quad [3.18a]$$

Although this transient heat transfer skews the overall room heat balance results, the effect is minimal.

One other condition is noted here. By inspection of Figures 3.3 -3.8, while both the room inlet and outlet temperatures appear to be decreasing, for the 5 ach experiments, the inlet temperature rate of decrease is greater than the room outlet. This indicates that the room inlet-to-outlet ΔT is increasing, thus increasing the overall air heat gain. It is not clear how long this trend continues but assuming the room were allowed to run for an additional 4 hours, for the 5 ach experiment, the room inlet would see a 14 °F decrease. While this may over-predict, the implication is clear that the room heat balance would have benefited from a longer run time.

3.3.4.2 *Room Conduction Backlosses*

As per the previous discussion, room stratification and room transient effects are responsible for some of the problems experienced at the lower volumetric flow rates. Additionally, room conduction backlosses, while negligible at the higher volumetric flow rates, begin to impact the heat balance at the lower volumetric flow rates. Table 3.8 shows a steady-state calculation of these conduction backlosses for all six surfaces. The lab room temperature is assumed to be approximately 70°F, which agrees well with hand measurements. Thus for R-67 walls and R-47 floor and ceiling, the conduction heat losses are as follows for the seven core experiments.

Table 3.8 Room Conduction Backlosses

code	ach	q _{cond} (btu/hr)
E012895A(1)	18	92.0
E022595B(2)	25	76.2
E030495(3)	23	57.1
E050695A(4)	8	178.4
E050695B(5)	23	55.6
E050695C(6)	6	194.9
E080595A(7)	25	46.7
E080595B(8)	6	144.2
E081295A(9)	24	45.2
E081295B(10)	1	178.8
E082695(11)	26	32.3
E090995(12)	25	42.7
E091695(13)	20	51.5
E091795A(14)	10	118.7
E091795B(15)	15	61.1
E091795C(16)	5	166.0
E110495(17)	5	178.0

3.3.5 Modified Heat Balance Results

As per the preceding discussion, the overall heat balance equation should be modified as follows for a given time period:

$$Q_{\text{air},i} = \Sigma Q_{\text{panel},i} - \Sigma Q_{\text{cond},i} - \Sigma Q_{\text{trans},i} \quad [3.19]$$

For the 5 ach experiment (E091795C), referring to Table 3.5, the total energy out is calculated as follows (Here, Q_{air} has been revised based on a correction of the inlet temperature computed in section 3.3.3.2.):

$$Q_{\text{out}} = Q_{\text{air}} + Q_{\text{cond}} + Q_{\text{trans}}$$

$$Q_{\text{out}} = 3042 + 166 + 30 = 3238 \text{ btu/hr} \quad [3.20]$$

With the revised uncertainty a modified heat balance plot for the 5 ach experiment is obtained in Figure 3.11. This is a plot of energy in versus energy out treating the experimental room as the control volume. Once again the line $y=x$ represents the ideal heat balance. Here, the heat balance is shown to be within the estimated uncertainty.

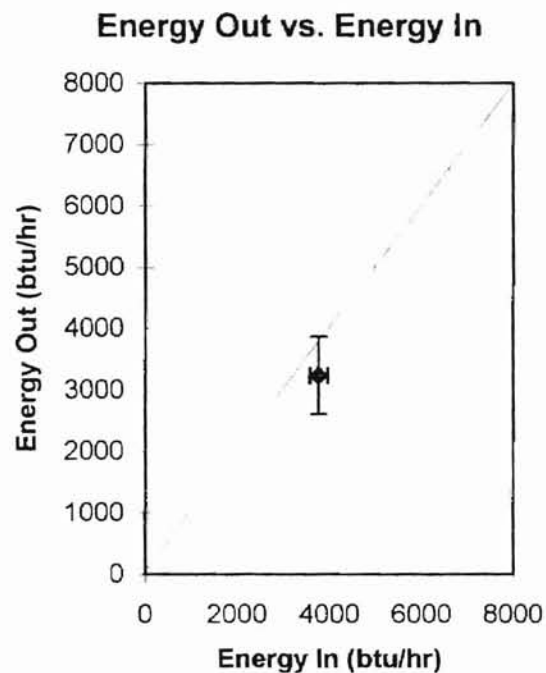


Figure 3.11 Modified Heat Balance - Energy Out vs. Energy In (5 ach)

In summary, the following complicating factors have been discussed and have been shown to have an adverse effect on the room heat balance:

1. Inlet gradient effect, which skews the inlet temperature measurement
2. Radiation effects on the inlet temperature
3. Transient effects

4. Conduction backloss effects

For the 5 ach test, the errors may be ranked in order of significance (approximate % error in the heat balance):

1. Radiation effects (7.8%)
2. Conduction effects (5.1%)
3. Transient effects (1.0%)
4. Inlet gradient effects (0.3%)

Additionally, it should be noted that only 12 of the proposed 70 heated panels have been installed for the initial tests. Especially at the lower flow rates, increased room power, resulting in increased conduction backlosses, will have an appreciable effect on the room heat balance. This can be mitigated by completing the guard space and its heating system.

Finally, the room inlet temperature gradient effect was minimal and could be reduced to negligible values by providing both a more uniform flow of air at the room inlet and reducing the room inlet cross-section. Further experimentation should focus on these factors to improve the overall room heat balance and thus improve the facility performance.

CHAPTER FOUR - SUMMARY AND RECOMMENDATIONS

An experimental facility for the study of interior convective heat transfer in buildings has been designed, constructed and tested at Oklahoma State University. The facilities' flexibility makes it a one-of-a-kind full scale structure for the study of convective heat transfer. Building on previous work by Spitler et. al. at the University of Illinois Urbana-Champaign, the following is a list of measures taken in the design of the facility to improve overall performance and usefulness:

1. Use of a modular heated panel system to allow flexible inlet and outlet configurations.
2. Increased cooling capacity via a water source heat pump and chilled water tank.
3. Elevated floor of room for environmental control of all six facility surfaces.
4. Increased overall and incremental supply of air to room via ASHRAE Standard 51 Outlet Chamber Setup. This design provided numerous nozzle configurations allowing for flow rates from 5 to 100 ACH.

Initial experiments focused on heated panel control and room heat balance. The heated panels performed best at low air flow rates and were shown to be under-powered at higher flow rates (> 15 ach) for the current panel control strategy. An analysis of inlet and outlet temperatures versus time indicated that the room was not at a true steady state temperature condition. However, for the purposes of overall facility heat balance performance, the averaging period was deemed quasi-steady state. The room heat balance results indicated, that at higher flow rates, agreeable heat balance results were obtained. However, at the lower volumetric flow rates, room transient effects, errors in inlet room

temperature measurement, and room conduction backlosses combined to adversely affect heat balance results. These uncertainties were difficult to quantify and further experimentation is recommended to investigate and reduce the uncertainties. For the study at hand time constraints did not allow a full investigation of these issues.

At the lower volumetric flow rates, errors in the inlet temperature measurement were caused by a vertical temperature gradient in the inlet and radiation to the thermocouples. The overall accuracy of inlet temperature measurement should be improved as this was a considerable source of heat balance uncertainty.

Overall facility performance and usefulness could be improved markedly with the implementation of the following measures:

1. Install radiation shields for thermocouples to reduce radiation error of temperature measurement.
2. Allow room to stabilize by increasing run times to approximately 8 hours from start of fan.
3. Finish installation of controlled guard space to diminish conduction backlosses.
4. Reduce inlet cross-sectional area and/or install settling means for more uniform airflow.
5. Modify panel control algorithm to obtain a panel duty cycle of 100%.
6. Install reheat coil system for variable room inlet temperature control.
7. Increase fan and air measurement box capacity.
8. Increase panel power and the number of heated panels.
9. Implement an electronic pressure measurement system, thereby reducing averaging errors caused by manual manometer readings.
10. Increase sample size for spatially averaged quantities (i.e., panel, inlet, outlet, and room temperatures), thereby reducing uncertainties.

11. Provide for variable fan operation to increase supply air volume control.
12. Implement a velocity measurement system.
13. Install a real-time panel voltage measurement system.
14. Refine overall room radiation analysis.

With these measures implemented, combined with the facilities' flexibility, the following list summarizes potential projects and investigations for this facility:

1. Determination of convection coefficients for interior building heat transfer in a full scale facility.
2. Radiant panel heating system investigations.
3. Attic and plenum heat transfer investigations.
4. Radiant and convective fractions of various internal load sources.
5. Simulation of glazing systems.
6. Convective heat transfer dependence on wall roughness.
7. Numerous inlet/outlet configuration and flow regime studies.

BIBLIOGRAPHY

- Akbari, H., D. Samano, A. Mertol, F. Bauman, and R. Kammerud, 1986, *The Effect of Variations in Convection Coefficients on Thermal Energy Storage in Buildings Part I - Interior Partition Walls*, Energy and Buildings, Vol. 9, pp. 195-211.
- Akbari, H., D. Samano, A. Mertol, F. Bauman, and R. Kammerud, 1987, *The Effect of Variations in Convection Coefficients on Thermal Energy Storage in Buildings Part II - Exterior Massive Walls and Simulations*, Energy and Buildings, Vol. 10, pp. 29-47.
- Bauman, F., A. Gadgil, R. Kammerud, E. Altmayer, and M.W. Nansteel, 1982, *Convective Heat Transfer in Buildings: Recent Research Results*, LBL Technical Report 13883, October 1982.
- Bauman, F. A. Gadgil, R. Kammerud, and R. Greif, 1980, *Buoyancy-Driven Convection in Rectangular Enclosures: Experimental Results and Numerical Calculations*, ASME 80-HT-66 19th National Heat Transfer Conference, Orlando, Florida.
- Chen, Q., and Van der Kooi, J., 1987, *Experiments and 2D Approximated Computations of 3D Air Movement, Heat and Concentration Transfer in a Room*, RoomVent-87 Air Distribution in Ventilated Spaces, Stockholm, Sweden.
- Fisher, D.E., 1989, Design of an Experimental Facility for the Investigation of Convective Heat Transfer in Enclosures, Masters Thesis, University of Illinois at Urbana-Champaign.
- Gadgil, A., F. Bauman, R. Kammerud, and K. Ruberg, 1980, *Natural Convection in Room Geometries*, Proceedings AS/ISES Solar Jubilee, June.
- Gadgil, A., F. Bauman, and R. Kammerud, 1982, *Natural Convection in Passive Solar Buildings: Experiments, Analysis, and Results*, *Passive Solar Journal*, Vol.1, No.1, pp. 28-40.
- Khalifa, A.J.N. and R.H. Marshall, 1989, *Natural and Forced Convection on Interior Building Surfaces: Preliminary Results*, Applied Energy Research Conference, Swansea.
- Parker, J.D., J.H. Boggs, E.F. Blick, 1972, Introduction to Fluid Mechanics and Heat Transfer, Addison-Wesley.
- Sanders, S., 1992, An Experimental Facility for Studying Convective Heat Transfer in Buildings, Masters Thesis, Oklahoma State University
- Siegel, R, and J.R. Howell, 1974, Thermal Radiation Heat Transfer, McGraw-Hill.
- Spitler, J.D., 1990, An Experimental Investigation of Air Flow and Convective Heat Transfer in Enclosures Having Large Ventilative Flow Rates, Doctoral Thesis, University of Illinois at Urbana-Champaign.

Spitler, J.D., C.O. Pedersen, D.E. Fisher, P.F. Menne, and J. Cantillo, 1991, *An Experimental Facility for Investigation of Interior Convective Heat Transfer*, ASHRAE Transactions, Vol.97, Pt.1, pp. 497-504.

Spitler, J.D., C.O. Pedersen, and D.E. Fisher, 1991, *Interior Convective Heat Transfer in Buildings with Large Ventilative Flow Rates*, ASHRAE Transactions, Vol.97, Pt.1, pp. 505-515.

Spitler, J.D., C.O. Pedersen, and R.J. Bunkofske, 1987, *Experimental Study of Interior Convective and Radiative Heat Transfer in Buildings*, Heat Transfer in Building and Structures, ASME HTD Vol.78, pp. 67-76.

Van der Kooi, J.K.B., 1983, *Improvement of Cooling Load Programs by Measurements in a Climate Room with Mass*, Proceedings of the XVIth International Congress of Refrigeration, pp. 54-60, Paris.

Walton, G.N., 1982, *Airflow and Multiroom Thermal Analysis*, ASHRAE Transactions, Vol.88, Pt.2, pp. 78-91.

Weber, D.D., 1980, Similitude Modeling of Natural Convection Heat Transfer Through an Aperture in Passive Solar Heated Buildings, Doctoral Thesis, University of Idaho.

Welty, J.R., C.E. Wicks, R.E. Wilson, 1969, Fundamentals of Momentum, Heat, and Mass Transfer, John Wiley & Sons.

Zhang, J.S., L.L. Christianson, G.J. Wu, and G.L. Riskowski, 1989, *An Experimental Study of Flow Regime in Mechanically Ventilated Spaces*, 1989 Proceedings of Joint Summer Meeting - ASAE/CSAE, Quebec, Canada.

Zhang, J.S., G.J. Wu, and L.L. Christianson, 1993, *A New Similitude Modeling Technique for Studies of Nonisothermal Room Ventilation Flows*, ASHRAE Transactions, Vol.99, Pt.1.

APPENDICES

Appendix A.

Data Analysis Program

```

DECLARE SUB avgdata ()
DECLARE SUB nzldata ()

```

```

=====
'Assign global data types to variables and arrays
=====

```

```

COMMON SHARED pretext AS STRING
COMMON SHARED timertext AS STRING
COMMON SHARED text1 AS STRING
COMMON SHARED text2 AS STRING
COMMON SHARED context AS STRING
COMMON SHARED control1 AS INTEGER
COMMON SHARED int1 AS INTEGER
COMMON SHARED int2 AS INTEGER
COMMON SHARED int3 AS INTEGER
COMMON SHARED control2 AS INTEGER
COMMON SHARED filenum AS INTEGER
COMMON SHARED volt AS SINGLE
COMMON SHARED R AS SINGLE
COMMON SHARED resist AS SINGLE
COMMON SHARED rhor AS SINGLE
COMMON SHARED rhoi AS SINGLE
COMMON SHARED rhoo AS SINGLE
COMMON SHARED rhonzl AS SINGLE
COMMON SHARED pb AS SINGLE
COMMON SHARED pe AS SINGLE
COMMON SHARED pp AS SINGLE
COMMON SHARED re3 AS SINGLE
COMMON SHARED re7 AS SINGLE
COMMON SHARED c3 AS SINGLE
COMMON SHARED c7 AS SINGLE
COMMON SHARED mdot AS SINGLE
COMMON SHARED qin AS SINGLE
COMMON SHARED qout AS SINGLE
COMMON SHARED alpha AS SINGLE
COMMON SHARED y AS SINGLE
COMMON SHARED a3 AS SINGLE
COMMON SHARED a7 AS SINGLE
COMMON SHARED d3 AS SINGLE
COMMON SHARED d7 AS SINGLE
COMMON SHARED pi AS SINGLE
COMMON SHARED cp AS SINGLE
COMMON SHARED bal AS SINGLE
COMMON SHARED ach AS SINGLE
COMMON SHARED volume AS SINGLE
COMMON SHARED index1 AS INTEGER
COMMON SHARED index2 AS INTEGER
COMMON SHARED count AS SINGLE
COMMON SHARED maincount AS INTEGER
COMMON SHARED sumup AS INTEGER
COMMON SHARED tracker AS INTEGER
COMMON SHARED qinavg AS SINGLE
COMMON SHARED qoutavg AS SINGLE

```

```
COMMON SHARED panelsum1 AS SINGLE
COMMON SHARED panelsum2 AS SINGLE
COMMON SHARED nzlsum1 AS SINGLE
COMMON SHARED nzlsum2 AS SINGLE
COMMON SHARED nzlsum3 AS SINGLE
COMMON SHARED swllsum1 AS SINGLE
COMMON SHARED swllsum2 AS SINGLE
COMMON SHARED nwllsum1 AS SINGLE
COMMON SHARED nwllsum2 AS SINGLE
COMMON SHARED ewllsum1 AS SINGLE
COMMON SHARED ewllsum2 AS SINGLE
COMMON SHARED risum1 AS SINGLE
COMMON SHARED risum2 AS SINGLE
COMMON SHARED risum3 AS SINGLE
COMMON SHARED rosum1 AS SINGLE
COMMON SHARED rosum2 AS SINGLE
COMMON SHARED rosum3 AS SINGLE
COMMON SHARED clgsum1 AS SINGLE
COMMON SHARED clgsum2 AS SINGLE
COMMON SHARED flrsum1 AS SINGLE
COMMON SHARED flrsum2 AS SINGLE
COMMON SHARED riavg AS SINGLE
COMMON SHARED roavg AS SINGLE
COMMON SHARED nzlavg AS SINGLE
COMMON SHARED swllavg AS SINGLE
COMMON SHARED nwllavg AS SINGLE
COMMON SHARED ewllavg AS SINGLE
COMMON SHARED clgavg AS SINGLE
COMMON SHARED flravg AS SINGLE
COMMON SHARED panelavg AS SINGLE

DIM SHARED pnltemps(1 TO 500, 1 TO 12) AS SINGLE
DIM SHARED clgtemps(1 TO 500, 1 TO 6) AS SINGLE
DIM SHARED flrtemps(1 TO 500, 1 TO 6) AS SINGLE
DIM SHARED swlltemps(1 TO 500, 1 TO 6) AS SINGLE
DIM SHARED nwlltemps(1 TO 500, 1 TO 6) AS SINGLE
DIM SHARED ewlltemps(1 TO 500, 1 TO 3) AS SINGLE

DIM SHARED nzltemps(1 TO 500, 1 TO 4) AS SINGLE
DIM SHARED rotemps(1 TO 500, 1 TO 4) AS SINGLE
DIM SHARED ritemps(1 TO 500, 1 TO 4) AS SINGLE
DIM SHARED contint(1 TO 500, 1 TO 12) AS INTEGER
DIM SHARED setpoint(1 TO 17) AS INTEGER
DIM SHARED config(1 TO 17) AS INTEGER
DIM SHARED upper(1 TO 17) AS INTEGER
DIM SHARED lower(1 TO 17) AS INTEGER
DIM SHARED deltap(1 TO 17) AS SINGLE
DIM SHARED code(1 TO 17) AS INTEGER
DIM SHARED nzlavg1(1 TO 50) AS SINGLE
DIM SHARED riavg1(1 TO 50) AS SINGLE
DIM SHARED roavg1(1 TO 50) AS SINGLE
DIM SHARED nzlavg3(1 TO 500) AS SINGLE
DIM SHARED riavg3(1 TO 500) AS SINGLE
DIM SHARED roavg3(1 TO 500) AS SINGLE
```

```

DIM SHARED clgavg1(1 TO 50) AS SINGLE
DIM SHARED flravg1(1 TO 50) AS SINGLE
DIM SHARED nwillavg1(1 TO 50) AS SINGLE
DIM SHARED swllavg1(1 TO 50) AS SINGLE
DIM SHARED ewllavg1(1 TO 50) AS SINGLE
DIM SHARED panelavg1(1 TO 50) AS SINGLE
DIM SHARED counter(1 TO 50) AS SINGLE
DIM SHARED instbal(1 TO 50) AS SINGLE
DIM SHARED vdot(1 TO 50) AS SINGLE
DIM SHARED qin(1 TO 50) AS SINGLE

CLS

FOR i = 1 TO 17
  READ setpoint(i), config(i), upper(i), lower(i), deltapi(i), code(i)
NEXT i

FOR k = 1 TO 17

filenum = FREEFILE

'=====
'Initialize counters and assign constants
'=====

volt = 121.6
resist = 79.5
pb = 29.92
cp = .245
volume = 12! * 10! * 16!
R = 53.35
pi = 3.1416
d16 = 1.6 / 12!
d3 = 3! / 12!
d7 = 7! / 12!
a16 = pi * d16 ^ 2 / 4
a3 = pi * d3 ^ 2 / 4
a7 = pi * d7 ^ 2 / 4
index1 = 0
index2 = 0
qintot = 0
sumup = 0
tracker = 1
maincount = 0

'=====
'Open data files for batch input
'=====

SELECT CASE code(k)
CASE 1
  OPEN "c:\thesis\datfiles\p012895a.dat" FOR INPUT AS #filenum
CASE 2
  OPEN "c:\thesis\datfiles\le022595b.dat" FOR INPUT AS #filenum

```

```

CASE 3
  OPEN "c:\thesis\datfiles\le030495.dat" FOR INPUT AS #filenum
CASE 4
  OPEN "c:\thesis\datfiles\p050695a.dat" FOR INPUT AS #filenum
CASE 5
  OPEN "c:\thesis\datfiles\le050695b.dat" FOR INPUT AS #filenum
CASE 6
  OPEN "c:\thesis\datfiles\le050695c.dat" FOR INPUT AS #filenum
CASE 7
  OPEN "c:\thesis\datfiles\p080595a.dat" FOR INPUT AS #filenum
CASE 8
  OPEN "c:\thesis\datfiles\le080595b.dat" FOR INPUT AS #filenum
CASE 9
  OPEN "c:\thesis\datfiles\le081295a.dat" FOR INPUT AS #filenum
CASE 10
  OPEN "c:\thesis\datfiles\le081295b.dat" FOR INPUT AS #filenum
CASE 11
  OPEN "c:\thesis\datfiles\p082695.dat" FOR INPUT AS #filenum
CASE 12
  OPEN "c:\thesis\datfiles\le090995.dat" FOR INPUT AS #filenum
CASE 13
  OPEN "c:\thesis\datfiles\le091695.dat" FOR INPUT AS #filenum
CASE 14
  OPEN "c:\thesis\datfiles\le091795a.dat" FOR INPUT AS #filenum
CASE 15
  OPEN "c:\thesis\datfiles\le091795b.dat" FOR INPUT AS #filenum
CASE 16
  OPEN "c:\thesis\datfiles\le091795c.dat" FOR INPUT AS #filenum
CASE 17
  OPEN "c:\thesis\datfiles\le110495.dat" FOR INPUT AS #filenum
CASE ELSE
  PRINT "Invalid code number"
END SELECT

```

```

'=====
'Parse input files and assign all values to respective arrays
'=====

```

```

INPUT #filenum, pretext

```

```

FOR j = 1 TO upper(k)
  IF tracker = 1 THEN
    maincount = maincount + 1
    FOR i = 1 TO 12
      INPUT #filenum, pnltemps(maincount, i)
    NEXT i
    FOR i = 1 TO 6
      INPUT #filenum, clgtemps(maincount, i)
    NEXT i
    FOR i = 1 TO 6
      INPUT #filenum, flrtemps(maincount, i)
    NEXT i
    FOR i = 1 TO 6
      INPUT #filenum, swlltemps(maincount, i)
    NEXT i
  END IF
NEXT j

```

```

    ON ERROR GOTO 5
5  RESUME NEXT
  NEXT i
  FOR i = 1 TO 6
    INPUT #filenum, nwltemp(maincount, i)
  NEXT i
  FOR i = 1 TO 3
    INPUT #filenum, ewlltemp(maincount, i)
  NEXT i
  FOR i = 1 TO 4
    INPUT #filenum, nzltemp(maincount, i)
  NEXT i
  FOR i = 1 TO 4
    INPUT #filenum, rotemp(maincount, i)
  NEXT i
  FOR i = 1 TO 4
    INPUT #filenum, ritemp(maincount, i)
  NEXT i
  INPUT #filenum, timertext
  INPUT #filenum, counter
  INPUT #filenum, conttext
  INPUT #filenum, control1
  INPUT #filenum, control2
  FOR i = 1 TO 12
    INPUT #filenum, contint(maincount, i)
  NEXT i

  sumup = sumup + 1
  IF sumup = 3 THEN
    tracker = 1
    sumup = 0
  ELSE
    tracker = 0
  END IF
  GOTO 10

ELSE

=====
'Parse input files for averaging period only
=====

  FOR i = 1 TO 51
    INPUT #filenum, transdat
    ON ERROR GOTO 3
3  RESUME NEXT
  NEXT i
  INPUT #filenum, text1
  INPUT #filenum, count
  INPUT #filenum, text2
  INPUT #filenum, int1
  INPUT #filenum, int2
  FOR i = 1 TO 12
    INPUT #filenum, int3

```

```

NEXT i

sumup = sumup + 1
IF sumup < 3 THEN
  tracker = 0
ELSE
  tracker = 1
  sumup = 0
END IF
GOTO 10

END IF
10 NEXT j

CLOSE #filenum

CALL avgdata

'=====
'Open last six output files for transient nozzle, inlet and outlet data
'=====

IF code(k) >= 12 THEN
SELECT CASE code(k)
CASE 12
  OPEN "c:\thesis\output\090995.out" FOR OUTPUT AS #filenum
CASE 13
  OPEN "c:\thesis\output\091695.out" FOR OUTPUT AS #filenum
CASE 14
  OPEN "c:\thesis\output\091795a.out" FOR OUTPUT AS #filenum
CASE 15
  OPEN "c:\thesis\output\091795b.out" FOR OUTPUT AS #filenum
CASE 16
  OPEN "c:\thesis\output\091795c.out" FOR OUTPUT AS #filenum
CASE 17
  OPEN "c:\thesis\output\110495.out" FOR OUTPUT AS #filenum
CASE ELSE
  PRINT "Invalid code number"
END SELECT

'=====
'Print transient nozzle, inlet and outlet temperatures
'=====

FOR j = 1 TO maincount
  risum3 = 0
  rosum3 = 0
  nzlsum3 = 0
  FOR i = 1 TO 4
    risum3 = risum3 + ritemps(j, i)
    rosum3 = rosum3 + rotemps(j, i)
    nzlsum3 = nzlsum3 + nzltemps(j, i)
  NEXT i
  riavg3(j) = risum3 / 4

```



```

    roavg3(j) = rosum3 / 4
    nzlavg3(j) = nzlsum3 / 4

'   WRITE #filenum, nzlavg3(j), riavg3(j), roavg3(j)
   WRITE #filenum, nzltemps(j, 4), ritemps(j, 4), rotemps(j, 4)

NEXT j

CLOSE #filenum
END IF

=====
'Open last six output files for transient panel data
=====

IF code(k) >= 12 THEN
SELECT CASE code(k)
CASE 12
OPEN "c:\thesis\output\090995.pnl" FOR OUTPUT AS #filenum
CASE 13
OPEN "c:\thesis\output\091695.pnl" FOR OUTPUT AS #filenum
CASE 14
OPEN "c:\thesis\output\091795a.pnl" FOR OUTPUT AS #filenum
CASE 15
OPEN "c:\thesis\output\091795b.pnl" FOR OUTPUT AS #filenum
CASE 16
OPEN "c:\thesis\output\091795c.pnl" FOR OUTPUT AS #filenum
CASE 17
OPEN "c:\thesis\output\110495.pnl" FOR OUTPUT AS #filenum
CASE ELSE
PRINT "invalid code number"
END SELECT

=====
'Print transient panel data to file
=====

FOR j = 1 TO maincount

WRITE #filenum, pnltemps(j, 1), pnltemps(j, 2), pnltemps(j, 3), pnltemps(j, 4),
pnltemps(j, 5), pnltemps(j, 6), pnltemps(j, 7), pnltemps(j, 8),
pnltemps(j, 9), pnltemps(j, 10), pnltemps(j, 11), pnltemps(j, 12)

NEXT j
CLOSE #filenum
END IF

PRINT timertext
PRINT counter
PRINT conttext
PRINT control1, control2

```

```

*****
**** Calculation of volumetric flow rate ****
*****

pe = .000296 * nzlavg ^ 2 - .0159 * nzlavg + .41
pp = pe - pb((roavg - nzlavg) / 2700)
rhor = (70.73 * (pb - .378 * pp)) / (R * (roavg + 459.7))
rhoi = rhor * (roavg + 459.7) / (nzlavg + 459.7)

re7 = 1363000 * d7 * (deltap(k) * rhoi) ^ .5
re3 = 1363000 * d3 * (deltap(k) * rhoi) ^ .5
re16 = 1363000 * d16 * (deltap(k) * rhoi) ^ .5
c16 = .9866 - (7.006 / re16 ^ .5) + (134.6 / re16)
c3 = .9866 - (7.006 / re3 ^ .5) + (134.6 / re3)
c7 = .9866 - (7.006 / re7 ^ .5) + (134.6 / re7)

alpha = 1 - ((5.187 * deltap(k)) / (rhoi * R * (riavg + 459.7)))
y = 1 - (.548 * (1 - alpha))

SELECT CASE config(k)
CASE 1
vdot = 1096 * y * (deltap(k) / rhoi) ^ .5 * (c7 * a7)
CASE 2
vdot = 1096 * y * (deltap(k) / rhoi) ^ .5 * (c7 * a7 + c3 * a3 + c16 * a16)
CASE 3
vdot = 1096 * y * (deltap(k) / rhoi) ^ .5 * (c7 * a7 + c3 * a3)
CASE 4
vdot = 1096 * y * (deltap(k) / rhoi) ^ .5 * (c3 * a3 + c16 * a16)
CASE 5
vdot = 1096 * y * (deltap(k) / rhoi) ^ .5 * (c7 * a7 + c16 * a16)
CASE 6
vdot = 1096 * y * (deltap(k) / rhoi) ^ .5 * (c3 * a3)
CASE 7
vdot = 1096 * y * (deltap(k) / rhoi) ^ .5 * (c16 * a16)
CASE ELSE
PRINT "Invalid option number"
END SELECT

=====
'Calculate average air heat gain and panel power
=====

mdot = vdot * 60 * rhoi
IF code(k) = 10 THEN
qoutavg = mdot * cp * (roavg - nzlavg)
ELSE
qoutavg = mdot * cp * (roavg - riavg)
END IF
achact = vdot * 60 / volume

FOR i = 1 TO 50

addbit = 0

```

```

FOR j = 1 TO 12
  IF contint(i, j) = 0 THEN
    addbit = addbit + 0
  ELSE
    addbit = addbit + 1
  END IF
NEXT j

qin(i) = addbit * (volt ^ 2 / resist) * 3.412
qintot = qintot + qin(i)

NEXT i

qinavg = qintot / 50

IF qoutavg < qinavg THEN
  balavg = ((qinavg - qoutavg) / qinavg) * 100
ELSEIF qoutavg > qinavg THEN
  balavg = ((qoutavg - qinavg) / qoutavg) * 100
END IF

'=====
'Print averages to file
'=====

OPEN "c:\thesis\output\tempdata.out" FOR APPEND AS #filenum
IF code(k) = 1 THEN
  WRITE #filenum, "exp code", "Tnzl", "Tro", "Tri", "Tclg", "Tflr", "Tswll", "Tnwll", "Tewll"
END IF
WRITE #filenum, code(k), nzlavg, roavg, riavg, clgavg, flravg, swllavg, nwillavg, ewllavg
CLOSE #filenum

OPEN "c:\thesis\output\calcddata.out" FOR APPEND AS #filenum
IF code(k) = 1 THEN
  WRITE #filenum, "exp code", "Qpnl", "Qair", "Bal", "CFM", "ACH", "MDOT", "Tpnl"
END IF
WRITE #filenum, code(k), qinavg, qoutavg, balavg, vdot, achact, mdot, panelavg
CLOSE #filenum

NEXT k

'=====
'Input data for batch runs
'=====

DATA 105,2,986,936,.2,1
DATA 105,5,657,607,.52,2
DATA 105,1,926,876,.49,3
DATA 105,4,1040,990,1.09,4
DATA 105,1,774,724,.51,5
DATA 105,6,1213,1163,1.12,6
DATA 100,2,629,579,.4,7
DATA 100,6,547,497,1.12,8
DATA 98,1,1402,1352,.52,9

```

```

DATA 95,7,496,446,1.20,10
DATA 95,3,1004,954,.45,11
DATA 100,3,1380,1330,.45,12
DATA 100,1,1359,1309,.4,13
DATA 100,1,1232,1182,.1,14
DATA 100,1,620,570,.225,15
DATA 100,6,873,823,.75,16
DATA 100,6,714,664,.75,17

END

SUB avgdata
DIM i, j AS INTEGER

'OPEN filename$ FOR OUTPUT AS filename

panelsum2 = 0
nzlsum2 = 0
risum2 = 0
rosum2 = 0
nwllsum2 = 0
swllsum2 = 0
ewllsum2 = 0
firsum2 = 0
clgsum2 = 0

FOR j = 1 TO 50
panelsum1 = 0
nzlsum1 = 0
risum1 = 0
rosum1 = 0
nwllsum1 = 0
swllsum1 = 0
ewllsum1 = 0
firsum1 = 0
clgsum1 = 0

FOR i = 1 TO 4
risum1 = risum1 + ritemps(j, i)
nzlsum1 = nzlsum1 + nzltemps(j, i)
rosum1 = rosum1 + rotemps(j, i)
NEXT i

FOR i = 1 TO 6
nwllsum1 = nwllsum1 + nwlltemps(j, i)
firsum1 = firsum1 + firtemps(j, i)
clgsum1 = clgsum1 + clgtemps(j, i)
NEXT i

swllsum1 = swllsum1 + swlltemps(j, 1)
swllsum1 = swllsum1 + swlltemps(j, 2)
swllsum1 = swllsum1 + swlltemps(j, 3)
swllsum1 = swllsum1 + swlltemps(j, 6)

```

```
FOR i = 1 TO 12
  panelsum1 = panelsum1 + pnltmps(j, i)
NEXT i
```

```
FOR i = 1 TO 3
  ewllsum1 = ewllsum1 + ewlltmps(j, i)
NEXT i
```

```
riavg1(j) = risum1 / 4
roavg1(j) = rosum1 / 4
nzlavg1(j) = nzlsum1 / 4
nwllavg1(j) = nwllsum1 / 6
swllavg1(j) = swllsum1 / 4
ewllavg1(j) = ewllsum1 / 3
flravg1(j) = flrsum1 / 6
clgavg1(j) = clgsum1 / 6
panelavg1(j) = panelsum1 / 12
```

```
risum2 = risum2 + riavg1(j)
rosum2 = rosum2 + roavg1(j)
nzlsum2 = nzlsum2 + nzlavg1(j)
nwllsum2 = nwllsum2 + nwllavg1(j)
swllsum2 = swllsum2 + swllavg1(j)
ewllsum2 = ewllsum2 + ewllavg1(j)
flrsum2 = flrsum2 + flravg1(j)
clgsum2 = clgsum2 + clgavg1(j)
panelsum2 = panelsum2 + panelavg1(j)
```

```
NEXT j
```

```
riavg = risum2 / 50
roavg = rosum2 / 50
nzlavg = nzlsum2 / 50
nwllavg = nwllsum2 / 50
swllavg = swllsum2 / 50
ewllavg = ewllsum2 / 50
flravg = flrsum2 / 50
clgavg = clgsum2 / 50
panelavg = panelsum2 / 50
```

```
END SUB
```

Appendix B.

Air Side Equations for the Calculation of Volumetric Flow Rate

Air Density Equations:

$$p_e = 296 \times 10^{-4} t_{wo}^2 - 159 \times 10^{-2} t_{wo} + 0.41$$

$$p_p = p_b \left(\frac{t_{do} - t_{wo}}{2700} \right)$$

$$\rho_o = \frac{70.73(p_b - 0.378 p_p)}{R(t_{do} + 459.7)}$$

Chamber Air Density at Plane x:

$$\rho_x = \rho_o, \text{ for } P_{sx} < 4 \text{ in. wg.}$$

Fan Air Density:

$$\rho = \rho_o, \text{ for an outlet chamber setup}$$

Air Viscosity:

$$\mu = (11.00 + 0.018 t_d) \times 10^{-6}$$

Alpha Ratio:

$$\alpha = 1 - \frac{5.187 \Delta P}{\rho_x R(t_{ds} + 459.7)}$$

Beta Ratio:

$$\beta = 0, \text{ for chamber approach}$$

Expansion Factor:

$$Y = 1 - (0.548 + 0.71 \beta^4)(1 - \alpha)$$

Energy Factor:

$$E = 1.0, \text{ for chamber approach}$$

Reynolds Number:

$$Re = \frac{D_6 V_6 \rho_6}{60 \mu_6}$$

Reynolds Number Approximation:

$$Re = \frac{1096}{60 \mu_6} C D_6 Y \sqrt{\frac{\Delta P \rho_3}{1 - E \beta^4}}$$

Simplified Reynolds Number:

$$Re = 1,363,000 D_6 \sqrt{\frac{\Delta P \rho_3}{1 - \beta^4}}$$

$$C = 0.95, Y = 0.96, E = 1.0, \text{ and}$$

$$\mu = 1.222 \times 10^{-5} \text{ lbm/ft-s}$$

Discharge Coefficient:

$$C = 0.9986 - \frac{7.006}{\sqrt{Re}} + \frac{134.6}{Re}$$

for $l/d = 0.6$ & $Re \geq 12,000$

Flow Rate:

$$Q_5 = 1096Y \sqrt{\frac{\Delta P}{\rho_3}} \sum(CA_6),$$

Appendix C.

Dimensionless Parameters Overview

Archimedes Number

The Archimedes Number can be defined as the ratio of the buoyant forces to the inertial forces. The following equation is generally used:

$$Ar = \frac{\beta g L \Delta T}{U^2} \quad \text{where,} \quad [C-1]$$

L = length of enclosure (16 ft)

$\Delta T = T_o - T_i$ ($^{\circ}F$)

U_i = fluid inlet velocity (ft/s)

For a side wall inlet, from this formulation it can be deduced that for high Archimedes numbers buoyancy effects dominate and a natural convection flow condition exists. Conversely, for low Archimedes numbers inertial forces are dominant and forced convection flow is present. Physically speaking, the inlet jet enters the room and drops for high Archimedes numbers, whereas for low Archimedes numbers, the jet will travel across the room before finally diffusing or impinging upon a surface.

A variable of prime importance in this formulation is the characteristic length. Based upon an analysis by Spitler (1990), for a room of similar dimensions and inlet location, this characteristic length should be the distance from the room inlet to an opposite wall. Table 3.5 shows the variation in Archimedes numbers that were calculated for all seventeen experiments. It should be noted that this form of the Archimedes disregards viscous flow effects.

Reynolds Number

As reported by Spitler (1990), two forms of the Reynolds number are useful for this type of experimental setup. The two equations that follow express the Reynolds number in terms of inlet velocity and cross-sectional velocity both of which are reported in Table C.2.

$$\text{Re}_i = \frac{U_i * D_i}{\nu} \quad [\text{C-2}]$$

and

$$\text{Re}_x = \frac{U_\infty * D_x}{\nu} \quad \text{where,} \quad [\text{C-3}]$$

U_i = inlet fluid velocity (ft/s)

U_∞ = freestream velocity (ft/s) = \dot{V} / A_x

D_i = inlet diameter (ft)

D_x = equivalent room diameter (ft)

A_x = enclosure cross-sectional area (ft²)

Prandtl Number

The Prandtl number is defined as the ratio of the diffusion of momentum to the diffusion of heat. It is a function of fluid properties only and can be used to characterize the thermal and velocity boundary layers. For $\text{Pr} > 1$, the velocity boundary layer is thicker than the thermal boundary layer and the inverse is true

for $Pr < 1$. For $Pr = 1$, the relative thicknesses of both boundary layers is taken to be the same. Thus the velocity and temperature profiles are similar if the following boundary conditions apply:

$$\text{wall, } y = 0, u = 0, v = 0, t = t_w$$

$$\text{freestream, } y = \infty, u = u_\infty, t = t_\infty$$

This boundary layer relationship, as a result of boundary layer theory (Schlichting, 1968), can be expressed as follows:

$$\delta_V/\delta_T = Pr^{0.5} \quad [C-4]$$

Additionally, in equation form, the Prandtl number is expressed as follows:

$$Pr = \frac{\nu}{\alpha} = \frac{\mu c_p}{\kappa} \quad [C-5]$$

Grashof Number

The Grashof number represents the ratio of buoyancy forces to viscous forces. Thus for buoyancy driven flows, fluid velocities are determined by quantities in the Grashof number. In equation form:

$$Gr = \frac{\beta g \Delta T h^3}{\nu^2} \quad \text{where,} \quad [C-6]$$

h = height of enclosure (ft)

$$\Delta T = T_s - T_\infty \text{ (}^\circ\text{F)}$$

Rayleigh Number

The Rayleigh number is generally defined for enclosures with differential wall temperatures (Spitler, 1990). The Rayleigh number can be expressed as the product of the Pr and Gr numbers and is defined as the ratio of buoyant forces to viscous forces. Spitler suggests the following form:

$$Ra_{sj} = \frac{\beta g \Delta T h^3}{\nu \alpha} = Gr Pr \quad \text{where,} \quad [C-7]$$

h = height of enclosure (ft)

$\Delta T = T_s - T_i$ ($^{\circ}F$)

U_i = fluid inlet velocity (ft/s)

Jet Momentum Number

The Jet Momentum number, defined as the product of the mass flow rate and fluid inlet velocity, has been non-dimensionalized as follows (Barber, 1982):

$$J = \frac{\dot{V} * U}{g * V} \quad \text{where,} \quad [C-8]$$

\dot{V} = volumetric flow rate (ft^3/min)

U = fluid inlet velocity (ft/s)

V = enclosure volume (ft^3)

This form is potentially useful for analyzing ventilative flow patterns.

Table C.1 Dimensionless Parameters Matrix.

number	Gr	Pr	Ra	Re	Ar	J
equation	$\frac{\beta^* g^* \Delta T^* L^3}{\nu^2}$	$\frac{\nu}{\alpha}$	$\frac{\beta^* g^* \Delta T^* L^3}{\nu^* \alpha}$	$\frac{U^* D}{\nu}$	$\frac{\beta^* g^* \Delta T^* L}{U^2}$	$\frac{U^* Q}{g^* V}$
constants	g		g		g	g
properties	$(\mu, \rho, \beta)_{\infty}$	$(\mu, \rho, \kappa, c_p, \beta)_{\infty}$	$(\mu, \rho, \kappa, c_p, \beta)_{\infty}$	$\mu_{\infty}, \rho_{\infty}$ or μ_i, ρ_i	β_{∞}	ρ_i
ΔT	$T_{\text{surf}} - T_{\infty}$		$T_{\text{surf}} - T_i$		$T_{\infty} - T_i$	
L	h		h		l	
U				U_i or U_{∞}	U_i	U_i
D				D_i or D_{∞}		

Table C.2 Velocities and Dimensionless Parameters.

EXP	U_i (fpm)	U_∞ (fpm)	Re_i	Re_∞	Pr_i	Pr_∞	Gr_i	Gr_∞
1	257.63	6.02	45510	6573	0.6933	0.7089	1.14E+12	6.66E+11
2	356.50	8.32	62531	9133	0.6952	0.7078	1.07E+12	6.95E+11
3	328.77	7.68	58087	8492	0.6932	0.7055	1.12E+12	7.44E+11
4	114.50	2.67	20193	2857	0.6937	0.7151	1.15E+12	5.29E+11
5	334.06	7.80	59833	8692	0.6894	0.7035	1.23E+12	7.73E+11
6	90.53	2.11	15982	2249	0.6934	0.7162	1.16E+12	5.06E+11
7	364.65	8.51	65274	9556	0.6896	0.7015	1.12E+12	7.42E+11
8	90.48	2.11	15969	2273	0.6935	0.7132	1.04E+12	4.78E+11
9	337.47	7.88	60333	8829	0.6899	0.7020	1.08E+12	7.00E+11
10	26.54	0.62	4436	660	0.7086	0.7161	4.89E+11	3.12E+11
11	370.06	8.64	66718	9832	0.6876	0.6977	1.07E+12	7.43E+11
12	370.09	8.64	66689	9775	0.6877	0.6993	1.17E+12	7.88E+11
13	294.99	6.89	53020	7686	0.6884	0.7031	1.18E+12	7.13E+11
14	146.36	3.42	26064	3704	0.6910	0.7111	1.12E+12	5.25E+11
15	220.53	5.15	39644	5683	0.6884	0.7061	1.19E+12	6.40E+11
16	73.87	1.72	13039	1846	0.6935	0.7147	1.04E+12	4.41E+11
17	74.02	1.73	12856	1844	0.6980	0.7155	8.92E+11	4.20E+11

Table C.2 Dimensionless Parameters, Continued.

EXP	Ra_i	Ra_∞	Ra_{prgri}	$Ra_{prgr\infty}$	Ar	J
1	7.90E+11	4.72E+11	7.90E+11	4.72E+11	0.4325	6.509E-3
2	7.45E+11	4.98E+11	7.45E+11	4.92E+11	0.1865	1.246E-2
3	7.79E+11	5.31E+11	7.79E+11	5.25E+11	0.2119	1.060E-2
4	7.96E+11	3.84E+11	7.96E+11	3.78E+11	3.4809	1.286E-3
5	8.45E+11	5.51E+11	8.45E+11	5.44E+11	0.2399	1.094E-2
6	8.07E+11	3.68E+11	8.07E+11	3.63E+11	6.1961	8.036E-4
7	7.73E+11	5.27E+11	7.73E+11	5.21E+11	0.1690	1.304E-2
8	7.20E+11	3.45E+11	7.20E+11	3.41E+11	5.3319	8.029E-4
9	7.43E+11	4.97E+11	7.43E+11	4.91E+11	0.1987	1.117E-2
10	3.46E+11	2.24E+11	3.46E+11	2.23E+11	23.1251	6.907E-5
11	7.34E+11	5.23E+11	7.34E+11	5.19E+11	0.1428	1.343E-2
12	8.02E+11	5.57E+11	8.02E+11	5.51E+11	0.1600	1.343E-2
13	8.12E+11	5.08E+11	8.12E+11	5.01E+11	0.3168	8.533E-3
14	7.73E+11	3.80E+11	7.73E+11	3.73E+11	1.8800	2.101E-3
15	8.21E+11	4.60E+11	8.21E+11	4.52E+11	0.6720	4.769E-3
16	7.20E+11	3.20E+11	7.20E+11	3.15E+11	8.8740	5.350E-4
17	6.23E+11	3.04E+11	6.23E+11	3.00E+11	7.4783	5.373E-4

Appendix D.

Thermocouple Placement Inside Experimental Room

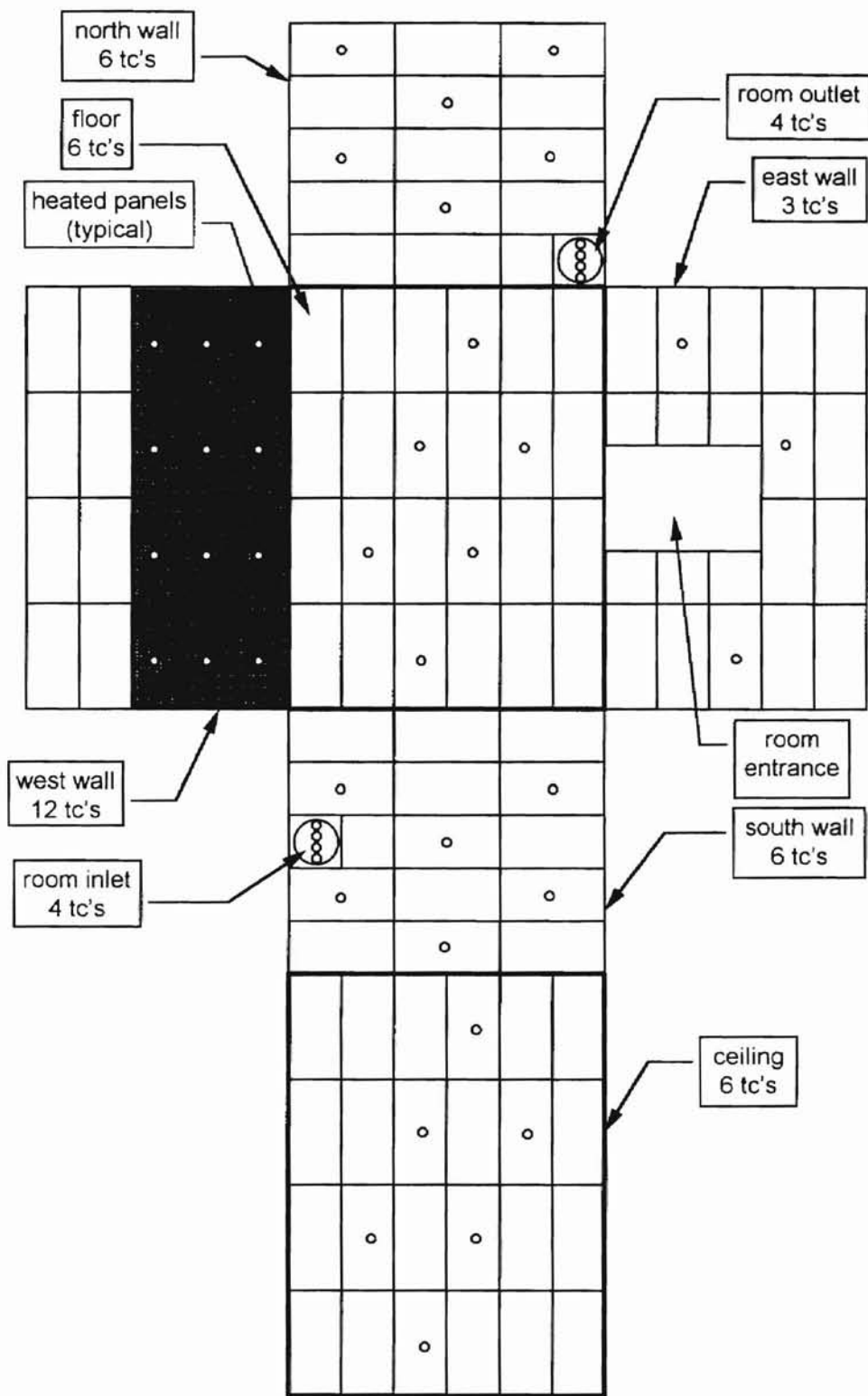


Figure D.1 Room Thermocouple Layout

Appendix E

Summary of Radiation View Factors

	tc	n	s	e	w	fl	clg	duct	pnl
tc		.12	0.0	.08	.05	.095	.08	.5	.075
n	.03		.128	.2	.08	.22	.22	.0024	.12
s	0.0	.136		.204	.086	.224	.224	0.0	.126
e	.01	.15	.147		.084	.24	.24	.003	.126
w	.017	.15	.16	.21		.23	.23	.003	0.0
fl	.06	.138	.14	.20	.08		.26	.002	.12
clg	.138	.138	.137	.20	.08	.26		.002	.12
duct	.001	.13	0.0	.20	.08	.22	.22		.15
pnl	.026	.15	.155	.18	0	.19	.21	.088	

Figure E.1 Summary of Radiant View Factors for Experimental Room

VITA

Jeffery D. Ferguson

Candidate for the Degree of

Master of Science

Thesis: A FULL SCALE ROOM FOR THE EXPERIMENTAL STUDY OF INTERIOR BUILDING CONVECTIVE HEAT TRANSFER: DESIGN AND VALIDATION

Major Field: Mechanical Engineering

Biographical:

Personal Data: Born in Elkhart, Kansas, On July 16, 1967, the son of Donnie and Karen Ferguson. Married Amy Turner on June 6, 1992. Jeff and Amy had their first child, Torie Dawn Ferguson, on May 17, 1993 and their second child, Taylor Elaine Ferguson, was born on December 25, 1994. Jeff and Amy currently reside in Owasso, OK.

Education: Graduated from Yarbrough High School, in May 1985; received a Bachelor of Science degree in Mechanical Engineering from Oklahoma State University, Stillwater, Oklahoma in May 1991. Completed the requirements for the Master of Science degree with a major in Mechanical Engineering at Oklahoma State University, in May 1997.

Experience: Jeff was raised in the Oklahoma Panhandle and worked summers on his grandfather's farm. Jeff was employed by the Department of Mechanical Engineering, Oklahoma State University as a research and teaching assistant, 1992-1993. Jeff accepted a position as an Engineering Project Coordinator at BSW International in June 1994, an architectural and engineering firm in Tulsa, Oklahoma, where he is presently employed.

Professional Memberships: American Society of Heating, Refrigerating and Air-Conditioning Engineers, American Society of Mechanical Engineering